Accepted Manuscript

Design, synthesis and biological evaluation of 2-(4-alkoxy-3-cyano)phenyl-6-oxo-1,6-dihydropyrimidine-5-carboxylic acid derivatives as novel xanthine oxidase inhibitors

Qing Mao, Xiwen Dai, Gaoyang Xu, Yu Su, Bing Zhang, Dan Liu, Shaojie Wang

PII: S0223-5234(19)30682-8

DOI: https://doi.org/10.1016/j.ejmech.2019.07.061

Reference: EJMECH 11558

To appear in: *European Journal of Medicinal Chemistry*

Received Date: 31 May 2019

Revised Date: 13 July 2019

Accepted Date: 21 July 2019

Please cite this article as: Q. Mao, X. Dai, G. Xu, Y. Su, B. Zhang, D. Liu, S. Wang, Design, synthesis and biological evaluation of 2-(4-alkoxy-3-cyano)phenyl-6-oxo-1,6-dihydropyrimidine-5-carboxylic acid derivatives as novel xanthine oxidase inhibitors, *European Journal of Medicinal Chemistry* (2019), doi: https://doi.org/10.1016/j.ejmech.2019.07.061.

Design, synthesis and biological evaluation of 2-(4-alkoxy-3-cyano)phenyl-6-oxo-1,6-dihydropyrimidine-5-carboxylic acid derivatives as novel xanthine oxidase inhibitors

Qing Mao [a], Xiwen Dai [a], Gaoyang Xu [b], Yu Su [b], Bing Zhang [a], Dan Liu [a], Shaojie Wang [a, *]

[a]*Key Laboratory of Structure-Based Drugs Design & Discovery of Ministry of Education, School of Pharmaceutical Engineering, Shenyang Pharmaceutical University, 103 Culture Road, Shenhe District, Shenyang 110016, China*

[b]*Department of Pharmacology, Shenyang Pharmaceutical University, No.103 103 Culture Road, Shenhe District, Shenyang, Liaoning110016, China*

*Corresponding authors.

Tel/Fax: +86-24-43520230, E-mail: sjwang_99@163.com (S. J. Wang);

Abstract

In our previous study, we reported a series of 1-hydroxy-2-phenyl-1*H*-imidazole-5-carboxylic acid derivatives that presented excellent *in vitro* xanthine oxidase (XO) inhibitory potency. To further investigate the structure-activity relationships of these compounds, the imidazole ring was transformed to a pyrimidine ring to design 2-(4-alkoxy-3-cyano)phenyl-6-oxo-1,6-dihydropyrimidine-5-carboxylic acids (**8a-8j**), 2-(4-alkoxy-3-cyano)phenyl-4-methyl-6-oxo-1,6-dihydropyrimidine-5-carboxylic acids (**9c, 9e, 9j, 9l**) and 2-(4-alkoxy-3-cyano)phenyl-6-imino-1,6-dihydropyrimidine-5-carboxylic acids (**10c, 10e, 10j, 10l**). These compounds exhibited remarkable *in vitro* XO inhibitory potency with IC_{50} values ranging from 0.0181 μM to 0.5677 μM. Specifically, compounds **10c** and **10e**, with IC_{50} values of 0.0240 μM and 0.0181 μM, respectively, emerged as the most potent XO inhibitors, and their potencies were comparable to that of febuxostat. Structure-activity relationship analysis revealed that the methyl group at 4-position of pyrimidine ring could damage the potency, and the XO inhibitory potency was maintained when carbonyl group was changed to an imino group. Lineweaver-Burk plot analysis revealed that the representative compound **10c** acted as a mixed-type inhibitor. A potassium oxonate induced hyperuricemia model in rats was chosen to further confirm the hypouricemic effect of compound **10c**, and the results showed that compound **10c (**5 mg/kg**)** was able to significantly lower the serum uric acid level. Furthermore, in acute oral toxicity study, no sign of toxicity was observed when the mice were administered with a single 2000 mg/kg oral dose of compound **10c.** These results suggested that compound **10c** was a potent and promising uric acid-lowing agent for the treatment of hyperuricemia.

Keywords: 1,6-Dihydropyrimidine-5-carboxylic acid; Xanthine oxidase inhibitor; Synthesis; Biological evaluation.

1. Introduction

Xanthine oxidase (XO) is a key enzyme in the purine metabolic pathway that catalyzes the oxidation of hypoxanthine to xanthine and eventually to the final product uric acid [1]. The overproduction of uric acid could lead to hyperuricemia, which has been established as the major etiologic factor in gout [2]. The human body accumulates purines externally through the intake of food and internally through the degradation of DNA and RNA molecules. Specifically, modern humans have dramatically increased the consumption of purine-rich foods, alcohol, and soft drinks sweetened with fructose, which can cause overproduction of hypoxanthine and eventually lead to overproduction of uric acid [3-4]. Moreover, the high expression of XO is associated with overproduction of uric acid [4]. Many evidences established that inhibition of XO can effectively reduce the level of uric acid, and XO inhibitors are used as uric acid-lowering drugs for the treatment of hyperuricemia and gout [5-8].

Allopurinol, a classical XO inhibitor, has been used to treat hyperuricemia for several decades. However, as a purine analog, allopurinol affects the metabolism of purines and leads to severe life-threatening side effects, including fulminant hepatitis, renal failure, and Stevens-Johnson syndrome [4], in some cases. Hence, there is a considerable need for developing nonpurine XO inhibitors with potent XO inhibitory activity and with fewer side effects to replace allopurinol. As a result, the discovery of novel nonpurine XO inhibitors has drawn extensive attention from the

pharmaceutical industry worldwide in recent years, and many nonpurine XO inhibitors with excellent potency, such as pyrazoles (e.g., Y-700) [5-6], selenazoles [7], isoxazoles [8], imidazoles [9], triazoles [10-11], thiazoles [12-13] and some flavone analogs [18-25], have been reported. As a result of these efforts, febuxostat was approved by the FDA in 2009 [26], and another nonpurine XO inhibitor, topiroxostat, was subsequently approved in 2013 [27]. They both showed a more potent and longer-lasting urate-lowering effect than allopurinol (**Fig. 1**). However, in 2019, the FDA added a boxed warning for increased risk for heart-related death with febuxostat, and the mechanism of cardiotoxicity caused by febuxostat is not clear [28-29]. Therefore, new nonpurine XO inhibitors are still urgently needed to fulfill the clinical requirement of treatment of hyperuricemia and gout [30].

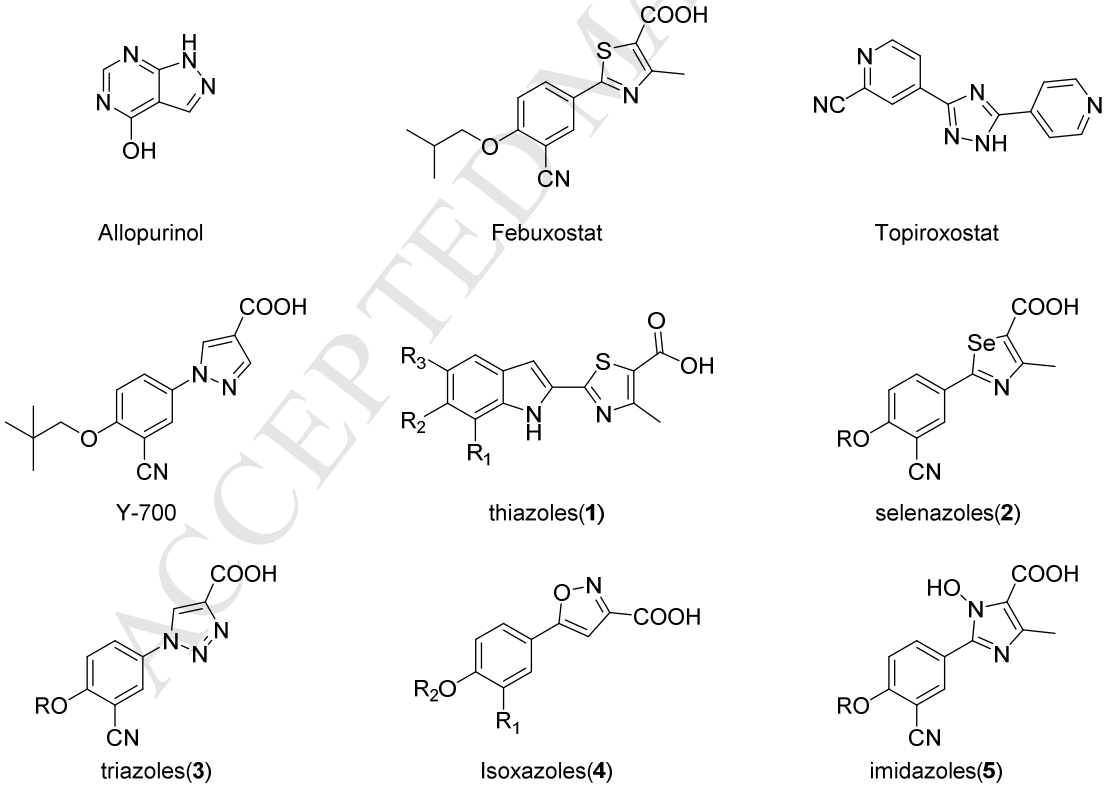

Fig. 1. Chemical structures of allopurinol and nonpurine XO inhibitors.

Pyrimidine is an important scaffold of many natural and synthetic products and is widely used in

medicinal chemistry [31-33]. In particular, Rao [34-36] and Narjes [37] have reported a series of pyrimidine-moiety containing XO inhibitors, such as compounds **6** and **7** (**Fig.2**), displaying excellent XO inhibitory potency. According to their docking research, the pyrimidine ring of compounds **6** and **7** as a whole is sandwiched between Phe914 and Phe1009 (face-to-face with Phe914 and face-to-edge with Phe1009) [34-37], and more interestingly, the same *pi*-stacking interaction could also be found in allopurinol with XO [38]. Therefore, the pyrimidine moiety could be used as a significant pharmacophore for XO inhibitor design. There are many successful cases of enlarging the five-membered heterocycles to corresponding six-membered ones in drug design [39-40], such as from fluvastatin to pitavastatin, in which enlargement of a pyrrole ring to a pyridine ring led to a significant improvement in potency [39]. The abovementioned findings encouraged us to enlarge the imidazole ring of 1-hydroxy-4-methyl-2-phenyl-1*H*-imidazole-5-carboxylic acids to a pyrimidine ring to design the 2-(4-alkoxy-3-cyano)phenyl-6-oxo-1,6-dihydropyrimidine-5-carboxylic acids as nonpurine XO inhibitors (**Fig. 2**). In addition, 4-methyl derivatives of 2-(4-alkoxy-3-cyano)phenyl-4-methyl-6-oxo-1,6-dihydropyrimidine-5-carboxylic acids and 2-(4-alkoxy-3-cyano)phenyl-6-imino-1,6-dihydropyrimidine-5-carboxylic acids were also designed for comparison.

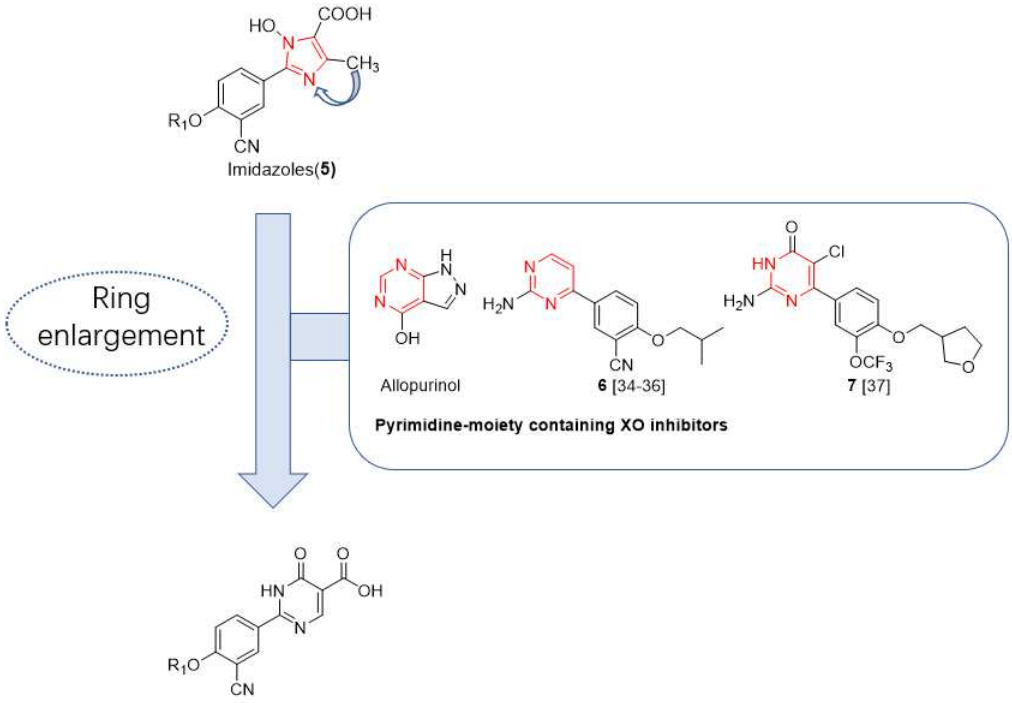

Fig. 2. Design of compounds.

In this study, we described the synthesis, *in vitro* XO inhibitory evaluation and structure-activity relationships (SARs) of 2-(4-alkoxy-3-cyano)phenyl-6-oxo-1,6-dihydropyrimidine-5-carboxylic acid derivatives, and molecular modeling studies and steady-state kinetic analysis were also performed to investigate the inhibitory behavior of the representative compound **10c**. Furthermore, the hypouricemic effect of **10c** was also evaluated using a potassium oxonate induced hyperuricemia model in rats. Finally, acute oral toxicity study of compound **10c** was performed according to OECD guidelines 2001 [41].

2. Results and discussion

2.1 Chemistry

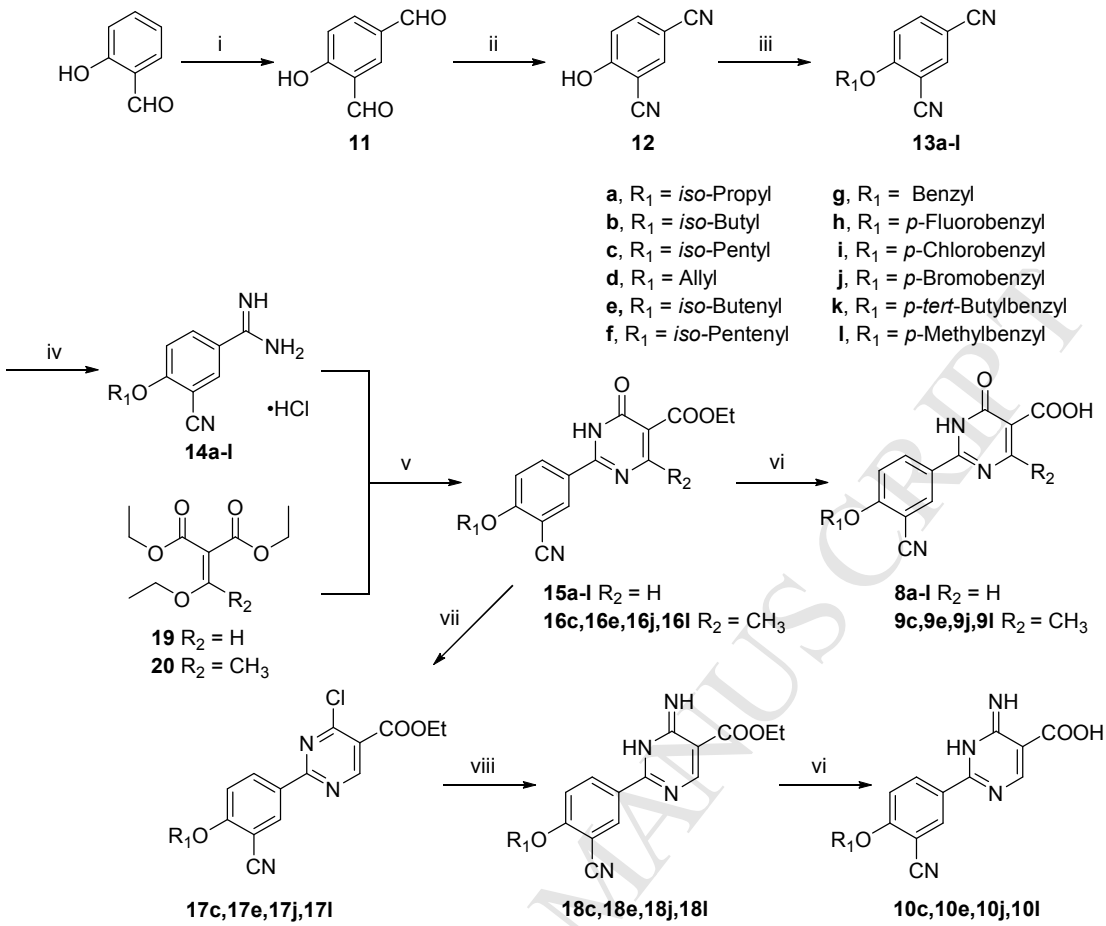

Scheme 1. Reagents and conditions: (i) a. hydrochloric acid, paraformaldehyde, $POCl_3$, rt, 8 h. b. HMTA, 50% CH_3COOH, reflux, 1 h. (ii) Hydroxylamine hydrochloride, HCOONa, HCOOH, NMP, reflux, 6 h. (iii) various alkyl chlorides or alkyl bromides, K_2CO_3, KI, DMF, 60°C, N_2. (iv) a. CH_3ONa, CH_3OH, rt, 24 h. b. NH_4Cl, 50°C, 4 h. (v) CH_3CH_2ONa, CH_3CH_2OH, 80°C, 2 h. (vi) LiOH, H_2O, THF, CH_3CH_2OH, 50°C, 3 h. (vii) $SOCl_2$, DMF, rt, 2 h. (viii) NH_4OH, THF, rt, 2 h.

The syntheses of the target compounds were performed as outlined in **Scheme 1**. The commercially available salicylaldehyde was chloromethylated with paraformaldehyde in hydrochloric acid to give 5-chloromethyl-2-hydroxybenzaldehyde, which was then transformed to 4-hydroxyisophthalaldehyde (**11**) via a Sommelet reaction [42]. Next, 4-hydroxyisophthalaldehyde (**11**) was treated with hydroxylamine hydrochloride to obtain the key intermediate

4-hydroxyisophthalonitrile (**12**) [43], which was alkylated with various alkyl halides to obtain the corresponding 4-alkoxy-isophthalonitriles (**13a-l**) with good yields [13]. Subsequently, 4-alkoxy-3-cyanobenzimidamide hydrochlorides (**14a-l**) were obtained through the alcoholysis of intermediate 4-alkoxy-isophthalonitriles (**13a-l**) in the presence of sodium methoxide followed by aminolysis with ammonium chloride [44]. Cyclization of diethyl ethoxymethylenemalonate (**19**) with 4-alkoxyisophthalonitriles (**14a-l**) in the presence of sodium ethoxide led to ethyl 2-(4-alkoxy-3-cyano)phenyl-6-oxo-1,6-dihydropyrimidine-5-carboxylates (**15a-l**) [45]. Finally, the target compounds, 2-(4-alkoxy-3-cyano)phenyl-6-oxo-1,6-dihydropyrimidine-5-carboxylic acids (**8a-l**), were obtained by hydrolyzing ethyl 2-(4-alkoxy-3-cyano)phenyl-6-oxo-1,6-dihydropyrimidine-5-carboxylates (**15a-l**) in an aqueous solution of lithium hydroxide. A similar method was used to synthesize 2-(4-alkoxy-3-cyano)phenyl-4-methyl-6-oxo-1,6-dihydropyrimidine-5-carboxylic acids (**9c, 9e, 9j, 9l**). The corresponding ethyl 2-(4-alkoxy-3-cyano)phenyl-6-imino-1,6-dihydropyrimidine-5-carboxylates (**18c, 18e, 18j, 18l**) were obtained through $SOCl_2$ chlorination of ethyl 2-(4-alkoxy-3-cyano)phenyl-6-oxo-1,6-dihydropyrimidine-5-carboxylates (**15c, 15e, 15j, 15l**) followed by ammonia aminolysis, and the 2-(4-alkoxy-3-cyano)phenyl-6-imino-1,6-dihydropyrimidine-5-carboxylic acids (**10c, 10e, 10j, 10l**) were synthesized by subsequently hydrolyzing the corresponding ethyl 2-(4-alkoxy-3-cyano)phenyl-6-imino-1,6-dihydropyrimidine-5-carboxylates (**17c, 17e, 17j, 17l**) in the aqueous solution of lithium hydroxide [45].

The target compounds were elucidated by HRMS, IR, ^{1}H NMR and ^{13}C NMR spectra. All

spectral data were in accordance with the assumed structures. In HRMS analysis, the target compounds showed $[M-H]^-$ ion peaks. The IR spectra of the target compounds displayed the cyano group stretching vibrations at 2239-2240 cm^{-1} and amide peaks at approximately 3406, 1645 and 1566 cm^{-1}. In ^1H NMR spectra, the CH of the pyrimidine ring was observed as a singlet at approximately 8.70 ppm for compounds **8a-l**. The singlet disappeared in 4-methyl derivatives **9c, 9e, 9j,** and **9l**.

2.2. XO inhibitory activity

The *in vitro* bovine XO inhibitory potencies of target compounds were measured spectrophotometrically by determining uric acid production at 295 nm [27]. Febuxostat and allopurinol were included as positive controls. As shown in **Table 1** and **Table 2**, all compounds exhibited excellent inhibitory potency with IC_{50} values ranging from 0.0181 µM to 0.5677 µM. In particular, the 6-imino derivatives **10c** (IC_{50} = 0.0240 µM) and **10e** (IC_{50} = 0.0181 µM), bearing an *iso*-pentyl and *iso*-butenyl substituent at R_1, respectively, emerged as the most potent XO inhibitors which were comparable to febuxostat (IC_{50} = 0.0236 µM), and their potencies were 316-fold and 419-fold higher than that of allopurinol, respectively.

Table 1

In vitro XO inhibitory potency of compounds **8a-l**

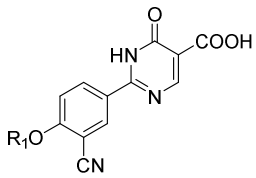

Compound	R_1	IC_{50} (μM) [a]	Compound	R_1	IC_{50} (μM) [a]
8a	*iso*-Propyl	0.0916 ± 0.0059	**8g**	Benzyl	0.0387 ± 0.0151
8b	*iso*-Butyl	0.0609 ± 0.0106	**8h**	*p*-Fluorobenzyl	0.0382 ± 0.0013
8c	*iso*-Pentyl	0.0250 ± 0.0066	**8i**	*p*-Chlorobenzyl	0.0499 ± 0.0098
8d	Allyl	0.0811 ± 0.0004	**8j**	*p*-Bromobenzyl	0.0298 ± 0.0093
8e	*iso*-Butenyl	0.0336 ± 0.0082	**8k**	*p*-*tert*-Butylbenzyl	0.1970 ± 0.0465
8f	*iso*-Pentenyl	0.0388 ± 0.0064	**8l**	*p*-Methylbenzyl	0.0354 ± 0.0075
Allopurinol		7.5902 ± 0.2145			
Febuxostat		0.0236 ± 0.0023			

[a] Values are means ± SD of three independent experiments

As shown in **Table 1**, the XO inhibitory potencies for the 2-(4-alkoxy-3-cyano)phenyl-6-oxo-1,6-dihydropyrimidine-5-carboxylic acids were influenced by the size of the carbon chain at R_1. The IC_{50} of compound **8c** (IC_{50} = 0.0250 μM), which bears an *iso*-pentyl substituent, was 3.7-fold and 2.4-fold higher than those of the *iso*-propyl and iso-butyl substituted compounds **8a** (IC_{50} = 0.0916 μM) and **8b** (IC_{50} = 0.0609 μM), respectively, which suggested that shortening the carbon chains could damage the potency. The IC_{50} value of the allyl-substituted compound **8d** was 0.0811 μM. Introducing a methyl substituent into the double bond of the allyl group led to compounds **8e** (IC_{50} = 0.0336 μM) and **8f** (IC_{50} = 0.0388 μM), and their potencies were 2.4-fold and 2.1-fold higher than that of **8d**, respectively. This finding indicated that the introduction of a methyl substituent into the double bond of the allyl group could favor the

XO inhibitory potency.

The benzyl substituted compound **8g** (IC_{50} = 0.0387 μM) showed a slight decrease in XO inhibitory potency compared with **8c**. To explore the possibility of improving the inhibitory activity of benzyl-substituted derivatives, a halogen (F, Cl and Br), methyl group and *tert*-butyl group were introduced at the *para*-position of the benzyl moiety. When a methyl group or a fluorine atom was linked at the *para*-position (**8l,** IC_{50} = 0.0354 μM and **8h**, IC_{50} = 0.0382 μM, respectively), the potency was maintained. Attachment of a bromine atom resulted in a slight increase in potency (**8j**, IC_{50} = 0.0298 μM). However, employment of a *tert*-butyl group at the *para*-position (**8k**, IC_{50} = 0.1970 μM) led to a significant decline in potency, and this decline is probably due to the steric hindrance created by the *tert*-butyl group. The above observations indicated that the bromine atom substituted at the *para*-position of the benzyl moiety was preferable for the potency.

Table 2

In vitro XO inhibitory potency of compounds **9c, 9e, 9j, 9l** and **10c, 10e, 10j, 10l**.

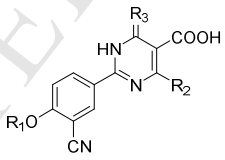

Compound	R_1	R_2	R_3	IC_{50} (μM) [a]
9c	*iso*-Pentyl	CH_3	O	0.5400 ± 0.0134
9e	*iso*-Butenyl	CH_3	O	0.5677 ± 0.0743
9j	*p*-Bromobenzyl	CH_3	O	0.1854 ± 0.0492
9l	*p*-Methylbenzyl	CH_3	O	0.1590 ± 0.0605
10c	*iso*-Pentyl	H	NH	0.0240 ± 0.0032
10e	*iso*-Butenyl	H	NH	0.0181 ± 0.0006

10j	*p*-Bromobenzyl	H	NH	0.0271 ± 0.0011
10l	*p*-Methylbenzyl	H	NH	0.0339 ± 0.0017
Allopurinol				7.5902 ± 0.2145
Febuxostat				0.0236 ± 0.0023

[a] Values are means ± SD of three independent experiments

Methyl groups play an important role in rational drug design [46]. A methyl group can modulate the physicochemical, pharmacodynamic and pharmacokinetic properties by the ortho effect [46]. Thus, we attempted to introduce a methyl group into the 4-position of the pyrimidine ring of compounds **8c**, **8e**, **8l** and **8j**, as the most potent compounds of 2-(4-alkoxy-3-cyano)phenyl-6-oxo-1,6-dihydropyrimidine-5-carboxylic acids, to obtain 4-methyl derivatives **9c**, **9e**, **9j**, and **9l** for comparison. As shown in **Table 2**, the introduction of a methyl group led to a 4.5-21.6-fold decrease in potency (**9c**, **9e**, **9j**, **9l** vs **8c**, **8e**, **8j**, **8l**). This finding suggested that the presence of a methyl group at the 4-position of the pyrimidine moiety could be detrimental to the potency.

The hydroxyl group of imidazole XO inhibitors acted as a hydrogen bond donor and linked to Thr1010 via a hydrogen bond [13]. Due to the amide-enamine tautomerism, the carbonyl group in the 6-position of the pyrimidine ring could function as a hydrogen bond acceptor or donor. Thus, we attempted to change the carbonyl group to an imino group, with the hope of maintaining the 6-position group as a hydrogen bond donor. Then, 2-(4-alkoxy-3-cyano)phenyl-6-imino-1,6-dihydropyrimidine-5-carboxylic acids (**10c, 10e, 10j** and **10l**) were synthesized. As shown in **Table 2**, the testing results showed that these compounds were effective with IC_{50} values ranging from 0.0181 to 0.0339 μM, and the XO inhibitory potency

increased compared with the corresponding carbonyl compounds (**10c, 10e, 10j, 10l** vs **8c**, **8e**, **8j**, **8l**). In particular, compound **10c** (IC_{50} of 0.0240 μM) and **10e** (IC_{50} of 0.0181 μM) showed the best XO inhibitory potency of all the target compounds. Furthermore, a Lineweaver-Burk plot (**Fig. 3**) revealed that compound **10c** acted as a mixed-type inhibitor of XO, which was similar to imidazole XO inhibitors and febuxostat [13, 26].

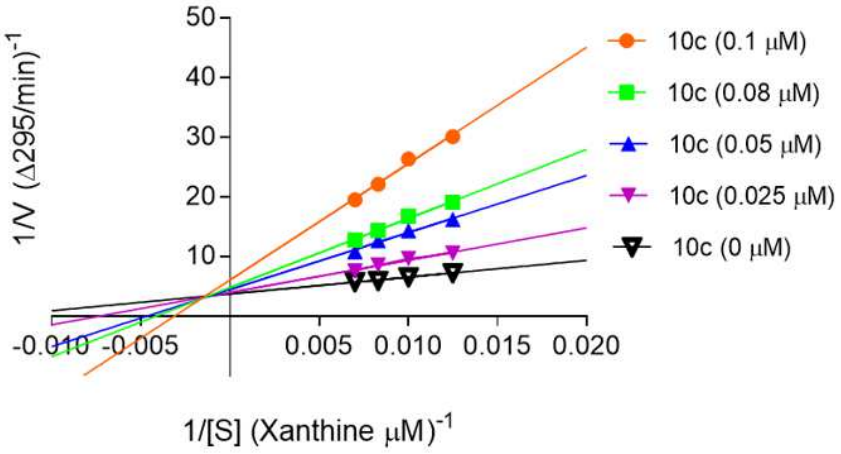

Fig. 3. Lineweaver-Burk plot analysis of xanthine oxidase by compound **10c**.

Furthermore, in order to obtain enzyme inhibition properties of compound **10c**, a kinetic analysis on the inhibition was performed using Lineweaver-Burk plot analysis. The Km and Vmax values were calculated as 75.72 μM and 0.0573 min^{-1} without the present of inhibitors, respectively. As show in **Fig.3**, in the presence of different concentrations of compound **10c** (0.025, 0.05, 0.08 and 0.1 μM), the apparent Km of enzyme was increased and the Vmax of the enzyme was decreased, thus compound **10c** inhibited the activity of XO through a mixed-type inhibition [22]. In a mixed-type inhibition, inhibitor can affect both the enzyme affinity for its substrate and the maximal rate of catalysis. The values of K_i (equilibrium constant for binding with free enzyme)

and K_{is} (equilibrium constant for binding with enzyme-substrate complex) were calculated to be 0.0042 μM and 0.1270 μM respectively, which confirmed that compound **10c** bound to the free XO much more easily and firmly than the XO-xanthine complex [23].

Table 3

Comparison of pyrimidines and imidazoles in XO inhibitory potency

Pyrimidines	R_1	RIP [a]	Imidazoles	R_1	RIP [a]
8a	*iso*-Propyl	3.85	**5a**	*iso*-Propyl	16.67
8b	*iso*-Butyl	2.56	**5b**	*iso*-Butyl	0.60
8c	*iso*-Pentyl	1.06	**5c**	*iso*-Pentyl	3.03
8j	*p*-Methylbenzyl	1.49	**5j**	*p*-Methylbenzyl	11.11

[a] Relative Inhibitory Potency (RIP) = $IC_{50\ compound}$ /$IC_{50\ febuxostat.}$

To compare the XO inhibitory potencies of 2-(4-alkoxy-3-cyano)phenyl-6-oxo-1,6-dihydropyrimidine-5-carboxylic acids (pyrimidine XO inhibitors) synthesized in this paper with those of 1-hydroxy-4-methyl-2-phenyl-1*H*-imidazole-5-carboxylic acids (imidazole XO inhibitors) synthesized before in our laboratory [13], the pyrimidines **8a**, **8b**, **8c** and **8j** together with the corresponding imidazoles **5a**, **5b**, **5c** and **5j** with the same R_1 groups were chosen. The relative inhibitory potency value [30] (RIP; the IC_{50} of a selected compound relative to the potency of febuxostat) was adopted as a comparison parameter. As shown in **Table 3,** the pyrimidine compounds showed relatively lower RIP values than those of imidazole compounds except the

iso-butyl substituted compound. These results suggested that the 6-oxo-1,6-dihydropyrimidine-5-carboxylic acid moiety was more favorable for the XO inhibitory potency than the 1-hydroxy-4-methyl-1*H*-imidazole-5-carboxylic acid moiety, and ring enlargement of the imidazole ring to a pyrimidine ring led to an increase in potency.

2.3. Molecular modeling

To explore the probable interaction model of inhibitors and the enzyme active site, molecular docking of the compounds **8c, 9c** and **10c** into the substrate binding pocket of XO was performed. The docking experiment was carried out using the Glide XP docking protocol (2016, Schrodinger Suite). Since molybdenum-pterion sites of both XO and xanthine dehydrogenase (XDH) are structurally equivalent [47], the X-ray crystal structure of the complex XDH/febuxostat (PDB code 1N5X) was adopted in the docking calculation [48]. The protein was prepared by removing all water molecules and adding all hydrogen atoms using Protein Preparation Wizard (2016, Schrodinger Suite). The carboxyl groups of the compounds **8c, 9c** and **10c** and febuxostat were calculated in dissociated form using the LIGPREP module in Schrodinger Suite. The binding models of the representative compounds **8c**, **9c** and **10c** were illustrated by Discovery Studio Visualizer 2017.

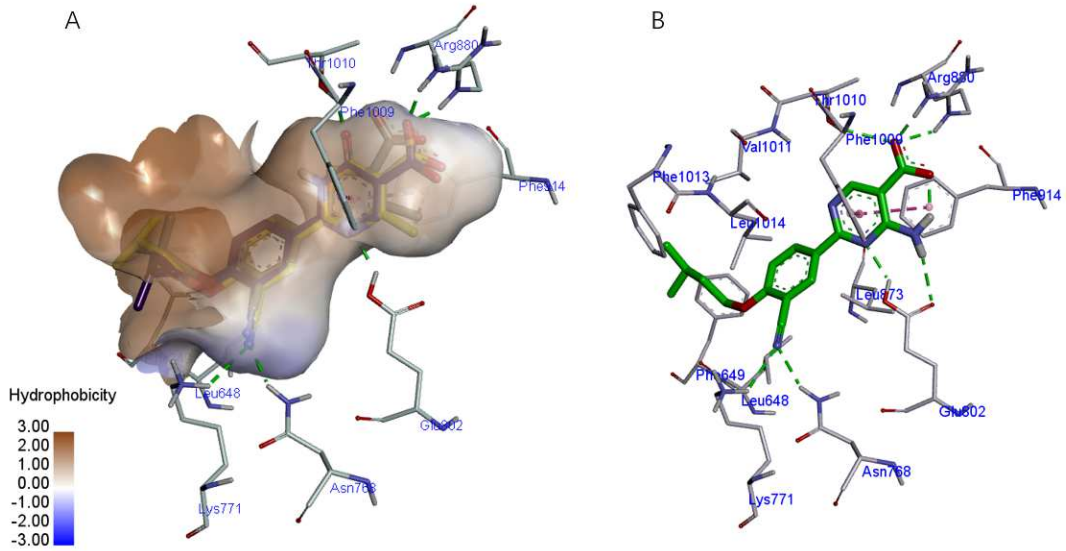

Fig. 4. Binding modes of compounds **8c**, **9c** and **10c** within the XO binding pocket. Hydrogen bonds are shown as green dashed lines, and π-π stacking interactions are shown as violet dashed lines. A) Overlay of compound **8c** (purple), **9c** (yellow) and febuxostat (gray) at the binding site. B) Binding modes of compound **10c** within the XO binding pocket.

As shown in **Fig. 4A**, compounds **8c** and **9c** presented a set of interactions similar to febuxostat. As expected, the pyrimidine ring as a whole was sandwiched between Phe914 and Phe1009 via face-to-face and face-to-edge *pi*-stacking interactions, respectively. In addition, the carbonyl group of the pyrimidine formed two hydrogen bonds with Thr1010, which was similar to the 1-hydroxyl group of the imidazole compound **5b** [13], the nitrogen atom of the pyrimidine forming a hydrogen bond with Glu802 and the cyano group of the phenyl unit forming a hydrogen bond with Asn768 and Lys771, and several hydrophobic interactions with Leu648, Phe649, Leu873, Val1011 and Leu1014 were also observed at the hydrophobic pocket. Moreover, we found that the methyl group at the 4-position of the pyrimidine ring was located on a hydrophilic surface (**Fig. 4A**), and the presence of a methyl group may adversely affect the activity. This observation explained the

decrease in activities after adding the methyl group at the 4-position of the pyrimidine ring.

The pyrimidine moiety of compound **10c** flipped 180 degrees (**Fig. 4B**), and the amino group established a hydrogen bond with the carboxyl group of Glu802 instead of forming a hydrogen bond with Thr1010, presenting a set of similar interactions to Rao's compound **6** [38-40]. Taking the potency comparison between the carbonyl series and imino series into consideration, we believe that the hydrogen bond formed between the amino group and Glu802 was stronger than that between the carbonyl group and Thr1010, and the interaction of the amino group with Glu802 could be highlighted for the design of novel nonpurine XO inhibitors.

2.4. Hypouricemic effect in vivo

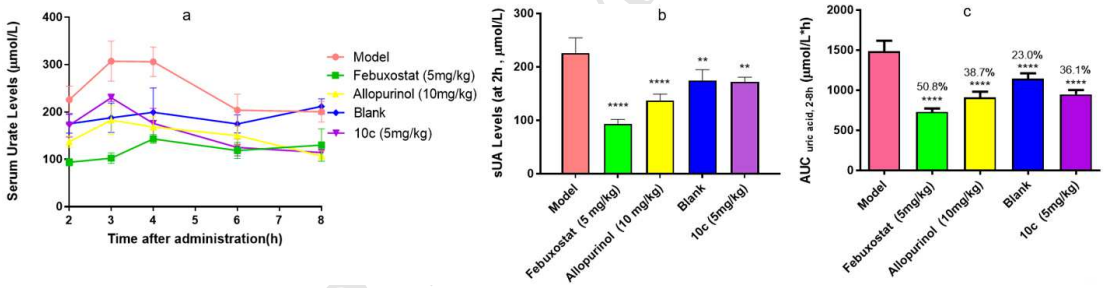

Fig. 5. Effect of compound **10c**, febuxostat and allopurinol on the serum uric acid levels in the potassium oxonate induced hyperuricemic rat model. (a) Time course changes in the serum uric acid levels after oral administration of compound **10c**, febuxostat and allopurinol in the potassium oxonate induced hyperuricemic rat model. (b) The sUA levels 2 h after oral administration of febuxostat, allopurinol and **10c** in the potassium oxonate induced hyperuricemic rat model. (c) The AUC (uric acid, 2-8 h) after oral administration of **10c**, febuxostat and allopurinol in the potassium oxonate induced hyperuricemic rat model. Data are expressed as the mean ± SD ****$P < 0.0001$, ** $P < 0.001$ vs hyperuricemic rats (model).

Compound **10c** was further tested *in vivo* to verify its hypouricemic effect in the acute hyperuricemic rat model compared to the standard inhibitors febuxostat and allopurinol by examining uric acid levels in the serum (**Fig. 5**). As expected, subcutaneous injection of 300 mg/kg potassium oxonate into rats markedly increased serum uric acid (sUA) levels in the hyperuricemia vehicle group compared to the blank group ($P < 0.001$ for **Blank** vs **Model**). At a single oral dose of 5 mg/kg, compound **10c** was able to significantly reduce the serum concentration of uric acid compared with the hyperuricemia vehicle group 2 h after administration in hyperuricemic rats ($P< 0.001$). In addition, the AUC of sUA levels from a 2 h to 8 h period of the study also showed that compound **10c** was able to significantly lower the sUA level compared with the model group ($P< 0.0001$), and the hypouricemic potency was similar to allopurinol (10 mg/kg). These results of *in vivo* hypouricemic activity evaluation suggested that compound **10c** was a potent and promising uric acid-lowering agent for the treatment of hyperuricemia.

2.5 Acute oral toxicity study

In order to explore the preliminary toxicity profile of the most potent compound **10c**, acute oral toxicity study was performed according to OECD guidelines 2001 [41], and the result showed that no gross behavioral abnormality was found within 24 h after the administration of test compound at a single dose of 2000 mg/kg, which suggested that LD_{50} value of compound **10c** might greater than 2000 mg/Kg, and it was about 400 times over the effective dose (5 mg/Kg). Thus, we can confirm that compound **10c** have good potential to be a safety and effective uric acid-lowing agent for the treatment of hyperuricemia.

3. Conclusion

In summary, we designed, synthesized and identified a series of 2-(4-alkoxy-3-cyano)phenyl-1,6-dihydropyrimidine-5-carboxylic acid derivatives as novel XO inhibitors, and these compounds showed excellent *in vitro* XO inhibitory potency. Specifically, compounds **10c** and **10e** emerged as the most potent XO inhibitors and were comparable to febuxostat. The potency comparison between the present pyrimidine compounds and the imidazole compounds reported before indicated that the 6-oxo-1,6-dihydropyrimidine-5-carboxylic acid moiety was more favorable for XO inhibitory potency than the 1-hydroxy-4-methyl-1*H*-imidazole-5-carboxylic acid moiety. SAR analysis revealed that the methyl group at the 4-position of the pyrimidine moiety could damage the potency, and an increasing trend could be observed when the carbonyl group was changed to an imino group. Molecular docking studies rationalized the SARs observed and provided insight into the binding mode of the target compounds with XO. Furthermore, the Lineweaver-Burk plot showed that the representative compound **10c** acted as a mixed-type XO inhibitor. The results of *in vivo* hypouricemic activity evaluation suggested that compound **10c** could considerably reduce the serum uric acid. Moreover, it was found noteworthy that no sign of toxicity was observed when the mice were administered with a single 2000 mg/kg oral dose of compound **10c**. Thus, these results suggested that compound **10c** was a potent and promising uric acid-lowering agent for the treatment of hyperuricemia.

4. Experimental protocols

4.1 Chemistry

Unless otherwise indicated, reagents and solvents were purchased from commercial sources and used without further purification. All reactions were monitored by TLC using silica gel aluminum cards (0.2 mm thickness) with 254 nm and 365 nm fluorescent indicators. Melting points were recorded on a YRT-3 melting apparatus and were uncorrected. ^{1}H NMR and ^{13}C NMR spectra were recorded on a Bruker 400 MHz or 600 MHz spectrometer. Chemical shifts were expressed in parts per million using tetramethylsilane as an internal reference and DMSO-d_6 as the solvent. IR spectra were determined as KBr pellets on a Bruker IFS-55 spectrometer and expressed as the number of wavelengths per centimeter. ESI-MS data were gathered using an Agilent 1100 instrument. ESI-HRMS data were recorded on the Agilent 6540 Series Q-TOF-MS system.

*4.1.1. Synthesis of 4-hydroxyisophthalaldehyde (**11**)*

A mixture of salicylaldehyde (60 g, 0.39 mol) and paraformaldehyde (24.2 g, 0.64 mol) in concentrated hydrochloric acid (390 ml) was stirred at room temperature for 1 h and then $POCl_3$ (20 ml) was added dropwise at 0 - 10 °C, large amounts of solids gradually precipitated. After completion of addition, the mixture was stirred at room temperature for another 8 h. The solid was separated by filtration as a white powder and dried under vacuum at 40 °C. The above product was

added to a solution of HMTA (74.7 g, 0.53 mol), H_2O (140 mL), CH_3COOH (140 mL) and refluxed for 1 h. After completion of the reaction, 140 ml of concentrated hydrochloric acid was added and refluxed for 10 min. Then, the mixture was poured into ice water and stirred for 30 min. The solid was separated by filtration as a yellow powder (66 g) in 89.5% yield which was used directly in the next step.

*4.1.2. Synthesis of 4-hydroxyisophthalonitrile (**12**)*

A solution of **11** (66 g, 0.44 mol), hydroxylamine hydrochloride (91.7 g, 1.32 mol), HCOONa (110.7 g, 1.63 mol), NMP (30 ml) in HCOOH (400 ml) was refluxed for 6 h. The reaction mixture was cooled at room temperature and stirred at 10 °C for 30 min. Then the precipitate was filtered and recrystallized from 50% ethanol to give **12** (34.5 g, 54.5%) as a gray white solid. mp: degraded at 190 °C. ^{1}H NMR (600 MHz, DMSO-d_6) δ 12.42 (s, 1H), 8.27 (s, 1H), 7.93 (d, J = 8.8 Hz, 1H), 7.15 (d, J = 8.8 Hz, 1H). ESI-MS: *m/z* 142.8 $[M-H]^-$.

*4.1.3. General procedure for the synthesis of 4-alkoxy-isophthalonitrile **13a-l***

A solution of **12** (50 mmol), anhydrous potassium carbonate (65 mmol), potassium iodide (1 mmol), and alkyl halide (75 mmol) in DMF (40 mL) was stirred at 50 °C for 6 h under nitrogen atmosphere. After the reaction was completed, the mixture was poured into water (200 mL). Then the precipitate was filtered and recrystallized from ethanol to yield 4-alkoxy- isophthalonitrile (**13a-l**).

*4.1.3.1. 4-iso-Propoxyisophthalonitrile(**13a**)*. A white solid, yield: 77.9%. mp: 147.9 °C – 148.5 °C.

^{1}H NMR (600 MHz, DMSO-d_6) δ 8.37 (s, 1H), 8.11 (d, *J* = 8.7 Hz, 1H), 7.47 (s, 1H), 4.95 (m, 1H), 1.35 (d, *J* = 5.9 Hz, 6H). ESI-MS: *m/z* 187.1 $[M+H]^+$.

*4.1.3.2. 4-iso-Butoxyisophthalonitrile(**13b**).* A white solid, yield: 88.1%. mp: 129.6 °C – 130.1 °C. ^{1}H NMR (600 MHz, DMSO-d_6) δ 8.36 (d, *J* = 2.1 Hz, 1H), 8.11 (dd, *J* = 8.9, 2.1 Hz, 1H), 7.42 (d, *J* = 8.9 Hz, 1H), 4.02 (d, *J* = 6.4 Hz, 2H), 2.07 (m, 1H), 1.00 (d, *J* = 6.7 Hz, 6H).。ESI-MS: *m/z* 223.8 $[M + Na]^+$.

*4.1.3.3. 4-iso-Pentyloxyisophthalonitrile(**13c**).* A white solid, yield: 66.6%. mp: 133.8 °C – 134.1 °C. ^{1}H NMR (600 MHz, DMSO-d_6) δ 8.36 (d, *J* = 2.1 Hz, 1H), 8.13 (dd, *J* = 8.9, 2.1 Hz, 1H), 7.45 (d, *J* = 8.9 Hz, 1H), 4.26 (t, *J* = 6.6 Hz, 2H), 1.79 (m, 1H), 1.66 (q, *J* = 6.7 Hz, 2H), 0.94 (d, *J* = 6.7 Hz, 6H). ESI-MS: *m/z* 215.7 $[M+H]^+$.

*4.1.3.4. 4-Allyloxyisophthalonitrile(**13d**).* A white solid, yield: 76.3%. mp: 200.4 °C – 201.1 °C. ^{1}H NMR (600 MHz, DMSO-d_6) δ 8.39 (d, *J* = 2.1 Hz, 1H), 8.14 (dd, *J* = 8.9, 2.1 Hz, 1H), 7.43 (d, *J* = 8.9 Hz, 1H), 6.06 (m, 1H), 5.47 (m, 1H), 5.34 (m, 1H), 4.86 (d, *J* = 5.2 Hz, 2H). ESI-MS: *m/z* 185.3 $[M+H]^+$.

*4.1.3.5. 4-(2-Methylallyloxy)isophthalonitrile(**13e**).* A white solid, yield: 73.3%. mp: 157.6 °C – 158.5 °C. ^{1}H NMR (600 MHz, DMSO-d_6) δ 8.41 (d, *J* = 2.2 Hz, 1H), 8.14 (dd, *J* = 8.9, 2.2 Hz, 1H), 7.43 (d, *J* = 8.9 Hz, 1H), 5.13 – 5.09 (m, 1H), 5.04 (t, *J* = 1.5 Hz, 1H), 4.78 (s, 2H), 1.79 (s, 3H). ESI-MS: *m/z* 199.1 $[M+H]^+$.

*4.1.3.6. 4-[(3-Methylbut-2-en-1-yl)oxy]isophthalonitrile(**13f**).* A white solid, yield: 61.2%. mp: 133.8 °C – 134.1 °C. ^{1}H NMR (600 MHz, DMSO-d_6) δ 8.37 (d, *J* = 2.2 Hz, 1H), 8.14 (dd, *J* = 8.9, 2.2 Hz, 1H), 7.44 (d, *J* = 8.9 Hz, 1H), 5.49 – 5.42 (m, 1H), 4.82 (d, *J* = 6.9 Hz, 2H), 1.76 (d, *J* = 15.9 Hz, 6H). ESI-MS: *m/z* 213.4 $[M+H]^+$.

*4.1.3.7. 4-Benzyloxyisophthalonitrile(**13g**).* A white solid, yield: 80.1%. mp: 184.6 °C – 185.7 °C. ^{1}H NMR (400 MHz, DMSO-d_6) δ 8.40 (d, *J* = 2.2 Hz, 1H), 8.15 (dd, *J* = 8.9, 2.2 Hz, 1H), 7.53 (d, *J* = 8.9 Hz, 1H), 7.51 – 7.34 (m, 5H), 5.40 (s, 2H). ESI-MS: *m/z* 235.4 $[M+H]^+$.

*4.1.3.8. 4-(4-Fluorobenzyloxy)isophthalonitrile(**13h**).* A white solid, yield: 43.8%. mp: 217.9 °C – 218.1 °C. ^{1}H NMR (400 MHz, DMSO-d_6) δ 8.41 (d, *J* = 2.1 Hz, 1H), 8.16 (dd, *J* = 8.8, 2.1 Hz, 1H), 7.64 (d, *J* = 8.1 Hz, 2H), 7.51 (d, *J* = 8.8 Hz, 1H), 7.45 (d, *J* = 8.1 Hz, 2H), 5.38 (s, 2H). ESI-MS: *m/z* 253.3 $[M+Na]^+$.

*4.1.3.9. 4-(4-Chlorobenzyloxy)isophthalonitrile(**13i**).* A white solid, yield: 43.6%. mp: 217.3 °C – 218.8 °C. ^{1}H NMR (400 MHz, DMSO-d_6) δ 8.41 (d, *J* = 2.2 Hz, 1H), 8.16 (dd, *J* = 8.9, 2.2 Hz, 1H), 7.72 – 7.60 (m, 2H), 7.51 (d, *J* = 8.9 Hz, 1H), 7.48 – 7.40 (m, 2H), 5.38 (s, 2H). ESI-MS: *m/z* 269.0 $[M+H]^+$.

*4.1.3.10. 4-(4-Bromobenzyloxy)isophthalonitrile(**13j**).* A white solid, yield: 86.2%. mp: 184.7 °C – 185.6 °C. ^{1}H NMR (400 MHz, DMSO-d_6) δ 8.41 (d, *J* = 2.2 Hz, 1H), 8.16 (dd, *J* = 8.9, 2.2 Hz, 1H),

7.64 (d, *J* = 8.0 Hz, 2H), 7.48 (m, 3H), 5.38 (s, 2H). ESI-MS: *m/z* 313.1 $[M+H]^+$.

*4.1.3.11. 4-[4-(tert-Butyl)benzyloxy]isophthalonitrile(**13k**).* A white solid, yield: 77.4%. mp: 133.3 °C – 133.9 °C. ^{1}H NMR (600 MHz, DMSO-d_6) δ 8.40 (d, *J* = 2.1 Hz, 1H), 8.16 (dd, *J* = 8.9, 2.1 Hz, 1H), 7.55 (d, *J* = 8.9 Hz, 1H), 7.46 (d, *J* = 8.4 Hz, 2H), 7.42 (d, *J* = 8.4 Hz, 2H), 5.36 (s, 2H), 1.29 (s, 9H). ESI-MS: *m/z* 291.4 $[M+H]^+$.

*4.1.3.12. 4-[(4-Methyl)benzyloxy]isophthalonitrile(**13l**).* A white solid, yield: 76.4%. mp: 174.5 ℃ – 175.9 °C. ^{1}H NMR (600 MHz, DMSO-d_6) δ 8.40 (d, *J* = 2.1 Hz, 1H), 8.15 (dd, *J* = 8.9, 2.1 Hz, 1H), 7.52 (d, *J* = 8.9 Hz, 1H), 7.37 (d, *J* = 8.0 Hz, 2H), 7.24 (d, *J* = 8.0 Hz, 2H), 5.35 (s, 2H), 2.32 (s, 3H). ESI-MS: *m/z* 249.2 $[M+H]^+$.

*4.1.4. General procedure for synthesis of 3-cyano-4-alkoxybenzimidamide hydrochloride(**14a-l**)*

A 500 mL flask was charged with anhydrous methanol (300 mL), compound **13a-l** (17.40 mmol) and sodium methoxide (5.22 mmol). The complex was protected from moisture and stirred for 36 h. Then, NH_4Cl (34.8 mmol) was added and stirring at 50°C for 6 h. Unreacted reactant was filtered, and the reaction mixture was concentrated under reduced pressure. The crude residue was refluxed with ethyl acetate and the precipitate was collected by filtration to give compounds **14a-l**, which was used for the next reaction without further purification.

*4.1.4.1. 3-Cyano-4-isopropoxybenzimidamide hydrochloride(**14a**).* A white solid, yield: 66.9%. mp: >250 °C. ^{1}H NMR (400 MHz, DMSO-d_6) δ 8.33 (d, *J* = 2.5 Hz, 1H), 8.20 (dd, *J* = 9.1, 2.5 Hz, 1H), 7.48 (d, *J* = 9.1 Hz, 1H), 4.97 (m, 1H), 1.37 (d, *J* = 5.9 Hz, 6H). ESI-MS: *m/z* 204.4 $[M+H]^+$.

*4.1.4.2. 3-Cyano-4-isobutoxybenzimidamide hydrochloride(**14b**).* A white solid, yield: 42.2%. mp: >250 °C. ^{1}H NMR (400 MHz, DMSO-d_6) δ 8.31 (d, *J* = 2.6 Hz, 1H), 8.18 (dd, *J* = 8.8, 2.6 Hz, 1H), 7.48 (d, *J* = 8.8 Hz, 1H), 4.06 (d, *J* = 6.4 Hz, 2H), 2.10 (m, 1H), 1.03 (d, *J* = 6.6 Hz, 6H). ESI-MS: *m/z* 218.1 $[M+H]^+$.

*4.1.4.3. 3-Cyano-4-isopentyloxybenzimidamide hydrochloride(**14c**).* A white solid, yield: 67.2%. mp: >250 °C. ^{1}H NMR (400 MHz, DMSO-d_6) δ 8.30 (d, *J* = 2.5 Hz, 1H), 8.17 (dd, *J* = 9.0, 2.5 Hz, 1H), 7.51 (d, *J* = 9.0 Hz, 1H), 4.30 (t, *J* = 6.5 Hz, 2H), 1.83 (m, 1H), 1.70 (q, *J* = 6.6 Hz, 2H), 0.96 (d, *J* = 6.6 Hz, 6H). ESI-MS: *m/z* 232.3 $[M+H]^+$.

*4.1.4.4. 4-Allyloxy-3-cyanobenzimidamide hydrochloride(**14d**).* A white solid, yield: 72.1%. mp: >250 °C. ^{1}H NMR (400 MHz, DMSO-d_6) δ 8.33 (d, *J* = 2.4 Hz, 1H), 8.19 (dd, *J* = 9.0, 2.4 Hz, 1H), 7.49 (d, *J* = 9.0 Hz, 1H), 6.09 (m, 1H), 5.55 – 5.44 (m, 1H), 5.37 (m, 1H), 4.89 (d, *J* = 5.2 Hz, 2H). ESI-MS: *m/z* 202.3 $[M+H]^+$.

*4.1.4.5. 3-Cyano-4-(2-methylallyloxy)benzimidamide hydrochloride(**14e**).* A white solid, yield: 68.1%. mp: >250 °C. ^{1}H NMR (600 MHz, DMSO-d_6) δ 8.38 (s, 1H), 8.21 (d, *J* = 9.2 Hz, 1H), 7.48 (d, *J* = 9.2 Hz, 1H), 5.11 (s, 1H), 5.03 (s, 1H), 4.80 (s, 2H), 1.79 (s, 3H). ESI-MS: *m/z* 216.2 $[M+H]^+$.

*4.1.4.6. 3-Cyano-4-[(3-methylbut-2-en-1-yl)oxy]benzimidamide hydrochloride(**14f**).* A white solid, yield: 41.1%. mp: >250 °C. ^{1}H NMR (600 MHz, DMSO-d_6) δ 8.34 (d, *J* = 2.4 Hz, 1H), 8.21 (dd, *J* =

9.0, 2.4 Hz, 1H), 7.48 (d, *J* = 9.0 Hz, 1H), 5.46 (t, *J* = 6.9 Hz, 1H), 4.82 (d, *J* = 6.8 Hz, 2H), 1.75 (dd, *J* = 10.5, 1.4 Hz, 6H). ESI-MS: *m/z* 230.3 $[M+H]^+$.

*4.1.4.7. 4-Benzyloxy-3-cyanobenzimidamide hydrochloride(**14g**).* A white solid, yield: 24.6%. mp: >250 °C. ^{1}H NMR (400 MHz, DMSO-d_6) δ 8.36 (d, *J* = 2.2 Hz, 1H), 8.12 (dd, *J* = 8.9, 2.2 Hz, 1H), 7.50 (d, *J* = 8.9 Hz, 1H), 7.41 (m, 5H), 5.37 (s, 2H). ESI-MS: *m/z* 252.4 $[M+H]^+$.

*4.1.4.8. 3-Cyano-4-(4-fluorobenzyloxy)benzimidamide hydrochloride(**14h**).* A white solid, yield: 58.3%. mp: >250 °C. ^{1}H NMR (400 MHz, DMSO-d_6) δ 8.34 (d, *J* = 2.5 Hz, 1H), 8.20 (dd, *J* = 9.0, 2.5 Hz, 1H), 7.65 – 7.52 (m, 3H), 7.28 (m, 2H), 5.41 (s, 2H). ESI-MS: *m/z* 270.2 $[M+H]^+$.

*4.1.4.9. 4-(4-Chlorobenzyloxy)-3-cyanobenzimidamide hydrochloride(**14i**).* A white solid, yield: 54.2%. mp: >250 °C. ^{1}H NMR (400 MHz, DMSO-d_6) δ 8.35 (d, *J* = 2.4 Hz, 1H), 8.21 (dd, *J* = 9.0, 2.4 Hz, 1H), 7.56 (m, 5H), 5.43 (s, 2H). ESI-MS: *m/z* 286.4 $[M+H]^+$.

*4.1.4.10. 4-(4-Bromobenzyloxy)-3-cyanobenzimidamide hydrochloride(**14j**).* A white solid, yield: 73.9%. mp: >250 °C. ^{1}H NMR (400 MHz, DMSO-d_6) δ 8.32 (d, *J* = 2.4 Hz, 1H), 8.16 (dd, *J* = 9.0, 2.4 Hz, 1H), 7.65 (d, *J* = 8.4 Hz, 2H), 7.56 (d, *J* = 9.0 Hz, 1H), 7.47 (d, *J* = 8.4 Hz, 2H), 5.41 (s, 2H). ESI-MS: *m/z* 332.1 $[M+H]^+$.

*4.1.4.11. 4-(4-tert-Butylbenzyloxy)-3-cyanobenzimidamide hydrochloride(**14k**).* A white solid, yield: 53.1%. mp: >250 °C. ^{1}H NMR (400 MHz, DMSO-d_6) δ 8.31 (d, *J* = 2.5 Hz, 1H), 8.15 (dd, *J* = 9.0,

2.5 Hz, 1H), 7.59 (d, *J* = 9.0 Hz, 1H), 7.51 – 7.38 (m, 4H), 5.38 (s, 2H), 1.29 (s, 9H). ESI-MS: *m/z* 308.4 $[M+H]^+$.

*4.1.4.12. 3-Cyano-4-(4-methylbenzyloxy)benzimidamide hydrochloride(**14l**).* A white solid, yield: 55.2%. mp: >250 °C. ^{1}H NMR (400 MHz, DMSO-d_6) δ 8.28 (d, *J* = 2.4 Hz, 1H), 8.12 (dd, *J* = 9.0, 2.4 Hz, 1H), 7.56 (d, *J* = 9.0 Hz, 1H), 7.39 (d, *J* = 8.0 Hz, 2H), 7.25 (d, *J* = 8.0 Hz, 2H), 5.37 (s, 2H), 2.32 (s, 3H). ESI-MS: *m/z* 266.4 $[M+H]^+$.

*4.1.5. General procedure for synthesis of ethyl 2-(4-alkoxy-3-cyanophenyl)-6-oxo-1,6-dihydropyrimidine-5-carboxylate(**15a-l**)*

Diethyl ethoxymethylenemalonate (4.6 mmol) were add to a solution of sodium hydride (9.7 mmol) and compound **14a-l** (4.2 mmol) in ethanol (20 mL), the reaction mixture was stirred at 80 °C for 2h. After the reaction completed, the mixture was added 10 mL 6 M hydrochloric acid and stirred for 0.5 h, then the precipitate was collected by filtration. The resulting residue was recrystallized from ethanol to yield ethyl 2-(4-alkoxyphenyl-3-cyano)-6-oxo-1,6-dihydropyrimidine-5-carboxylate(**15a-l**).

*4.1.5.1. Ethyl 2-(3-cyano-4-isopropoxyphenyl)-6-oxo-1,6-dihydropyrimidine-5-carboxylate (**15a**).* A white solid, yield: 43.1%. mp:199.8-201.1 °C. ^{1}H NMR (600 MHz, DMSO-d_6) δ 13.14 (s, 1H), 8.61 (s, 1H), 8.51 (d, *J* = 2.4 Hz, 1H), 8.46 – 8.40 (m, 1H), 7.45 (d, *J* = 9.2 Hz, 1H), 4.94 (hept, *J* = 6.0 Hz, 1H), 4.25 (q, *J* = 7.1 Hz, 2H), 1.36 (d, *J* = 6.0 Hz, 6H), 1.28 (t, *J* = 7.1 Hz, 3H). ESI-MS: *m/z* 350.7 $[M+Na]^+$.

*4.1.5.2. Ethyl 2-(3-cyano-4-isobutoxyphenyl)-6-oxo-1,6-dihydropyrimidine-5-carboxylate (**15b**).* A white solid, yield: 51.3%. mp: 207.5-209.8 ℃. ^{1}H NMR (600 MHz, DMSO-d_6) δ 13.16 (s, 1H), 8.61 (s, 1H), 8.52 (d, *J* = 2.4 Hz, 1H), 8.44 (d, *J* = 7.9 Hz, 1H), 7.42 (d, *J* = 9.1 Hz, 1H), 4.25 (q, *J* = 7.1 Hz, 2H), 4.03 (d, *J* = 6.6 Hz, 2H), 2.15 – 2.05 (m, *J* = 6.6 Hz, 1H), 1.29 (t, *J* = 7.1 Hz, 3H), 1.02 (d, *J* = 6.6 Hz, 6H). ESI-MS: *m/z* 342.4 $[M+H]^+$.

*4.1.5.3. Ethyl 2-(3-cyano-4-isopentyloxyphenyl)-6-oxo-1,6-dihydropyrimidine-5-carboxylate (**15c**).* A white solid, yield: 35.0%. mp: 190.7-193.4 ℃. ^{1}H NMR (600 MHz, DMSO-d_6) δ 13.17 (s, 1H), 8.63 (s, 1H), 8.53 (d, *J* = 2.4 Hz, 1H), 8.46 (d, *J* = 9.1 Hz, 1H), 7.47 (d, *J* = 9.1 Hz, 1H), 4.26 (M, 4H), 1.82 (m, *J* = 6.6 Hz, 1H), 1.69 (q, *J* = 6.6 Hz, 2H), 1.28 (t, *J* = 7.1 Hz, 3H), 0.96 (d, *J* = 6.6 Hz, 6H). ESI-MS: *m/z* 378.6 $[M+Na]^+$.

*4.1.5.4. Ethyl 2-(4-allyloxy-3-cyanophenyl)-6-oxo-1,6-dihydropyrimidine-5-carboxylate (**15d**).* A white solid, yield: 51.3%. mp: 209.3-210.7 ℃. ^{1}H NMR (600 MHz, DMSO-d_6) δ 13.18 (s, 1H), 8.64 (s, 1H), 8.55 (d, *J* = 2.3 Hz, 1H), 8.46 (d, *J* = 9.1 Hz, 1H), 7.45 (d, *J* = 9.1 Hz, 1H), 6.09 (m, 1H), 5.49 (m, 1H), 5.36 (m, 1H), 4.87 (d, *J* = 5.2 Hz, 2H), 4.26 (q, *J* = 7.1 Hz, 2H), 1.29 (t, *J* = 7.1 Hz, 3H). ESI-MS: *m/z* 347.8 $[M+Na]^+$.

*4.1.5.5. Ethyl 2-[3-cyano-4-(2-methylallyloxy)phenyl]-6-oxo-1,6-dihydropyrimidine-5-carboxylate (**15e**).* A white solid, yield: 62.5%. mp: 199.7-201.3 ℃. ^{1}H NMR (600 MHz, DMSO-d_6) δ 13.18 (s, 1H), 8.63 (s, 1H), 8.55 (d, *J* = 2.3 Hz, 1H), 8.50 – 8.38 (m, 1H), 7.43 (d, *J* = 9.1 Hz, 1H), 5.12 (s, 1H),

5.04 (s, 1H), 4.77 (s, 2H), 4.26 (q, *J* = 7.1 Hz, 2H), 1.81 (s, 3H), 1.29 (t, *J* = 7.1 Hz, 3H). ESI-MS: *m/z* 340.4 $[M+H]^+$.

4.1.5.6. Ethyl 2-[3-cyano-4-(3-methylbut-2-en-1-yl)oxyphenyl]-6-oxo-1,6-dihydropyrimidine-5-carboxylate ***(15f)***. A white solid, yield: 38.4%. mp: 204.3-205.9 ℃. ^{1}H NMR (600 MHz, DMSO-d_6) δ 13.17 (s, 1H), 8.63 (s, 1H), 8.53 (d, *J* = 2.3 Hz, 1H), 8.49 – 8.42 (m, 1H), 7.46 (d, *J* = 9.0 Hz, 1H), 5.49 (m, 1H), 4.82 (d, *J* = 6.8 Hz, 2H), 4.26 (q, *J* = 7.1 Hz, 2H), 1.77 (m, 6H), 1.29 (t, *J* = 7.1 Hz, 3H). ESI-MS: *m/z* 376.3$[M+Na]^+$.

*4.1.5.7. Ethyl 2-(4-benzyloxy-3-cyanophenyl)-6-oxo-1,6-dihydropyrimidine-5-carboxylate (**15g**).* A white solid, yield: 80.0%. mp: 215.7-217.9 ℃. ^{1}H NMR (600 MHz, DMSO-d_6) δ 13.17 (s, 1H), 8.62 (s, 1H), 8.55 (d, *J* = 2.4 Hz, 1H), 8.45 (d, *J* = 9.0 Hz, 1H), 7.54 (d, *J* = 9.1 Hz, 1H), 7.50 (d, *J* = 6.8 Hz, 2H), 7.44 (t, *J* = 7.6 Hz, 2H), 7.38 (t, *J* = 7.3 Hz, 1H), 5.40 (s, 2H), 4.25 (q, *J* = 7.1 Hz, 2H), 1.28 (t, *J* = 7.1 Hz, 3H). ESI-MS: *m/z* 376.3$[M+Na]^+$.

4.1.5.8. Ethyl 2-[3-cyano-4-(4-fluorobenzyloxy)phenyl]-6-oxo-1,6-dihydropyrimidine-5-carboxylate ***(15h)***. A white solid, yield: 46.9%. mp: 207.9-211.3 ℃. ^{1}H NMR (600 MHz, DMSO-d_6) δ 13.19 (s, 1H), 8.63 (s, 1H), 8.55 (d, *J* = 2.4 Hz, 1H), 8.47 (d, *J* = 9.0 Hz, 1H), 7.62 – 7.48 (m, 3H), 7.28 (t, *J* = 8.9 Hz, 2H), 5.39 (s, 2H), 4.26 (q, *J* = 7.1 Hz, 2H), 1.29 (t, *J* = 7.1 Hz, 3H). ESI-MS: *m/z* 394.2$[M+H]^+$.

4.1.5.9. *Ethyl 2-[3-cyano-4-(4-chlorobenzyloxy)phenyl]-6-oxo-1,6-dihydropyrimidine-5-carboxylate* ***(15i)***. A white solid, yield: 37.5%. mp: 226.1-227.7 ℃.^{1}H NMR (600 MHz, DMSO-d_6) δ 13.20 (s, 1H), 8.63 (s, 1H), 8.56 (d, *J* = 2.4 Hz, 1H), 8.46 (d, *J* = 9.0 Hz, 1H), 7.60 – 7.43 (m, 5H), 5.41 (s, 2H), 4.26 (q, *J* = 7.1 Hz, 2H), 1.29 (t, *J* = 7.1 Hz, 3H). ESI-MS: *m/z* 410.7[M+H] $^+$.

4.1.5.10. *Ethyl 2-[3-cyano-4-(4-bromobenzyloxy)phenyl]-6-oxo-1,6-dihydropyrimidine-5-carboxylate* ***(15j)***. A white solid, yield: 70.9%. mp: 221.4-223.5 ℃.^{1}H NMR (600 MHz, DMSO-d_6) δ 13.20 (s, 1H), 8.63 (s, 1H), 8.56 (d, *J* = 2.2 Hz, 1H), 8.46 (d, *J* = 9.1 Hz, 1H), 7.65 (d, *J* = 8.3 Hz, 2H), 7.57 – 7.39 (m, 3H), 5.39 (s, 2H), 4.26 (q, *J* = 7.1 Hz, 2H), 1.29 (t, *J* = 7.1 Hz, 3H). ESI-MS: *m/z* 476.9[M+Na] $^+$.

4.1.5.11. *Ethyl 2-[3-cyano-4-(4-tert-butylbenzyloxy)phenyl]-6-oxo-1,6-dihydropyrimidine-5-carboxylate* ***(15k)***. A white solid, yield: 66.1%. mp: 221.5-222.0 ℃. ^{1}H NMR (600 MHz, DMSO-d_6) δ 13.19 (s, 1H), 8.62 (s, 1H), 8.55 (d, *J* = 2.4 Hz, 1H), 8.46 (dd, *J* = 9.2, 2.4 Hz, 1H), 7.55 (d, *J* = 9.1 Hz, 1H), 7.49 – 7.41 (m, 4H), 5.35 (s, 2H), 4.26 (q, *J* = 7.1 Hz, 2H), 1.29 (m, 12H). ESI-MS: *m/z* 454.3[M+Na] $^+$.

4.1.5.12. *Ethyl 2-[3-cyano-4-(4-methylbenzyloxy)phenyl]-6-oxo-1,6-dihydropyrimidine-5-carboxylate* ***(15l)***. A white solid, yield: 44.4%. mp: 211.8-213.3 ℃.^{1}H NMR (600 MHz, DMSO-d6) δ 8.84 (s, 1H), 8.58 (d, J = 8.0 Hz, 2H), 7.52 (d, J = 1.6 Hz, 1H), 7.42 – 7.36 (m, 2H), 7.25 (d, J = 7.1 Hz, 2H), 5.32 (s,

2H), 4.32 (q, J = 7.1 Hz, 2H), 2.32 (s, 3H), 1.33 (t, J = 7.1 Hz, 3H).ESI-MS: *m/z* 390.3 $[M+H]^+$.

*4.1.6. General procedure for synthesis of ethyl 2-(4-alkoxy-3-cyanophenyl)-4-methyl-6-oxo-1,6-dihydropyrimidine-5-carboxylate (**16c, 16e, 16j, 16l**)*

Compounds **16c, 16e, 16j, 16l** were synthesized in the same manner as that for compounds **15a-l**, but using diethyl 2-(1-ethoxyethylidene)malonate instead of diethyl ethoxymethylenemalonate.

*4.1.6.1. Ethyl 2-(3-cyano-4-isopentyloxyphenyl)-4-methyl-6-oxo-1,6-dihydropyrimidine-5-carboxylate (**16c**).* A white solid, yield: 33.3%. mp: 168.5-172.7 ℃. ^{1}H NMR (600 MHz, DMSO-d_6) δ 13.05 (s, 1H), 8.47 (d, *J* = 2.3 Hz, 1H), 8.40 (d, *J* = 9.3 Hz, 1H), 7.44 (d, *J* = 9.1 Hz, 1H), 4.31 – 4.23 (m, 4H), 2.31 (s, 3H), 1.82 (m, 1H), 1.69 (q, *J* = 6.7 Hz, 2H), 1.28 (t, *J* = 7.1 Hz, 3H), 0.96 (d, *J* = 6.7 Hz, 6H). ESI-MS: *m/z* 370.4$[M+H]^+$.

*4.1.6.2. Ethyl 2-[3-cyano-4-(2-methylallyloxy)phenyl]-4-methyl-6-oxo-1,6-dihydropyrimidine-5-carboxylate (**16e**).* A white solid, yield: 37.3%. mp: 199.7-201.3 ℃. ^{1}H NMR (600 MHz, DMSO-d_6) δ 13.18 (s, 1H), 8.63 (s, 1H), 8.55 (d, *J* = 2.3 Hz, 1H), 8.50 – 8.38 (m, 1H), 7.43 (d, *J* = 9.1 Hz, 1H), 5.12 (s, 1H), 5.04 (s, 1H), 4.77 (s, 2H), 4.26 (q, *J* = 7.1 Hz, 2H), 2.39 (s, 3H), 1.81 (s, 3H), 1.29 (t, *J* = 7.1 Hz, 3H). ESI-MS: *m/z* 354.3$[M+H]^+$.

4.1.6.3. *Ethyl 2-[3-cyano-4-(4-bromobenzyloxy)phenyl]-4-methyl-6-oxo-1,6-dihydropyrimidine-5-carboxylate* ***(16j)***. A white solid, yield: 31.3%. mp: 199.7-203.3 ℃. ^{1}H NMR (600 MHz, DMSO-d_6) δ 13.04 (s, 1H), 8.46 (d, *J* = 2.3 Hz, 1H), 8.37 (d, *J* = 8.7 Hz, 1H), 7.63 – 7.60 (m, 2H), 7.49 – 7.46 (m, 1H), 7.43 (d, *J* = 8.1 Hz, 2H), 5.35 (s, 2H), 4.25 (q, *J* = 7.1 Hz, 2H), 2.28 (s, 3H), 1.25 (t, *J* = 7.1 Hz, 3H). ESI-MS: *m/z* 467.5 $[M+H]^+$.

4.1.6.4. *Ethyl 2-[3-cyano-4-(4-methylbenzyloxy)phenyl]-4-methyl-6-oxo-1,6-dihydropyrimidine-5-carboxylate* ***(16l)***. A white solid, yield: 35.6%. mp: 197.8-203.1 ℃. ^{1}H-NMR (400 MHz, DMSO-d_6) δ 8.54 (d, *J* = 2.3 Hz, 1H), 8.44 (dd, *J* = 9.0, 2.4 Hz, 1H), 7.55 (d, *J* = 9.1 Hz, 1H), 7.39 (d, *J* = 8.1 Hz, 2H), 7.24 (d, *J* = 8.0 Hz, 2H), 5.36 (s, 2H), 4.26 (q, *J* = 7.1 Hz, 2H), 2.65 (s, 3H), 2.32 (s, 3H), 1.29 (t, *J* = 7.1 Hz, 3H). ESI-MS: *m/z* 405.1$[M+H]^+$.

4.1.7. General procedure for synthesis of ethyl 2-(4-alkoxy-3-cyanophenyl)-4-chloropyrimidine-5-carboxylate ***(17c, 17e,17 j, 17l)***

A solution of ethyl 2-(4-alkoxy-3-cyanophenyl)-6-oxo-1,6-dihydropyrimidine-5-carboxylate and (0.013 mol), DMF (25 mL) was stirred at room temperature until clarified. Then $SOCl_2$ (0.0039 mol) was slowly added dropwise in 30 min. After addition, the mixture was stirred at room temperature for another 2h. The reaction solution was slowly poured into a 10% potassium carbonate solution (100 ml) at 0 °C and a large amount of solid was precipitated, stirred for 30 min, the resulting precipitate was filtered and dried to yield the corresponding ethyl

4-chloro-2-(4-alkoxy-3-cyanophenyl) pyrimidine-5-carboxylate.

*4.1.7.1. Ethyl 4-chloro-2-(3-cyano-4-isopentyloxyphenyl)pyrimidine-5-carboxylate (**17c**).* A white solid, yield: 77.3%. mp: degraded at 178.3 °C. ^{1}H NMR (600 MHz, DMSO-d6) δ 9.21 (s, 1H), 8.56 (dd, J = 9.0, 2.2 Hz, 1H), 8.52 (d, J = 2.3 Hz, 1H), 7.45 (d, J = 9.1 Hz, 1H), 4.39 (q, J = 7.1 Hz, 2H), 4.27 (t, J = 6.6 Hz, 2H), 1.84 (m, 1H), 1.70 (q, J = 6.7 Hz, 2H), 1.37 (t, J = 7.1 Hz, 3H), 0.97 (d, J = 6.7 Hz, 6H). ESI-MS: *m/z* 374.2[M+H] $^+$.

*4.1.7.2. Ethyl 4-chloro-2-[3-cyano-4-(2-methylallyloxy)phenyl]pyrimidine-5-carboxylate (**17e**).* A yellow solid, yield: 87.1%. mp: degraded at 179.9 °C. ^{1}H NMR (600 MHz, DMSO-d_6) δ 9.19 (s, 1H), 8.60 – 8.48 (m, 2H), 7.41 (d, *J* = 8.8 Hz, 1H), 5.08 (d, 2H), 4.73 (s, 2H), 4.37 (q, *J* = 7.1 Hz, 2H), 1.80 (s, 3H), 1.34 (t, *J* = 7.1 Hz, 3H). ESI-MS: *m/z* 358.3 [M+H] $^+$.

*4.1.7.3. Ethyl 2-[4-(4-bromobenzyloxy)-3-cyanophenyl]-4-chloropyrimidine-5-carboxylate (**17j**).* A white solid, yield: 88.9%. mp: degraded at 166.9 °C. ^{1}H NMR (600 MHz, DMSO-d_6) δ 9.25 (s, 1H), 8.66 – 8.60 (m, 2H), 7.71 – 7.63 (m, 2H), 7.55 (dd, *J* = 8.4, 1.1 Hz, 1H), 7.51 – 7.43 (m, 2H), 5.40 (s, 2H), 4.39 (q, *J* = 7.1 Hz, 2H), 1.36 (t, *J* = 7.1 Hz, 3H). ESI-MS: *m/z* 472.7[M+H] $^+$.

*4.1.7.4. Ethyl 4-chloro-2-[3-cyano-4-(4-methylbenzyloxy)phenyl]pyrimidine-5-carboxylate (**17l**).* A yellow solid, yield: 81.1% . mp: degraded at 177.7 °C. ^{1}H NMR (600 MHz, DMSO-d_6) δ 9.24 (s, 1H), 8.66 – 8.55 (m, 2H), 7.57 (dd, *J* = 8.7, 0.8 Hz, 1H), 7.40 (d, *J* = 8.0 Hz, 2H), 7.25 (d, *J* = 7.7 Hz, 2H), 5.36 (s, 2H), 4.39 (q, *J* = 7.1 Hz, 2H), 2.32 (s, 3H), 1.36 (t, *J* = 7.1 Hz, 3H). ESI-MS: *m/z* 408.3[M+H] $^+$.

*4.1.8. General procedure for synthesis of ethyl 2-(4-alkoxy-3-cyanophenyl)-6-imino-1,6-dihydropyrimidine-5-carboxylate (**18c, 18e, 18j, 18l**)*

A solution of ethyl 2-(4-alkoxy-3-cyanophenyl)-4-chloropyrimidine-5-carboxylate (0.01 mol), THF (20 mL) and concentrated aqueous ammonia (30 ml) was stirred at room temperature for 2 h. Then the reaction mixture was concentrated under reduced pressure, ethanol was added and stirred at room temperature for 1h, The resulting precipitate was filtered and dried to yield the corresponding 4-chloro-2-(4-alkoxy-3-cyanophenyl) pyrimidine-5-carboxylate.

*4.1.8.1. Ethyl 2-(3-cyano-4-isopentyloxyphenyl)-6-imino-1,6-dihydropyrimidine-5-carboxylate (**18c**).* A white solid, yield: 91.2%. mp: 108.1 – 109.7 °C. ^{1}H NMR (600 MHz, DMSO-d_6) δ 8.83 (s, 1H), 8.57 (dd, *J* = 8.9, 2.2 Hz, 1H), 8.55 (d, *J* = 2.2 Hz, 1H), 8.09 (s, 1H), 7.71 (s, 1H), 7.42 (d, *J* = 9.0 Hz, 1H), 4.32 (q, *J* = 7.1 Hz, 2H), 4.25 (t, *J* = 6.6 Hz, 2H), 1.83 (m, 1H), 1.69 (q, *J* = 6.7 Hz, 2H), 1.33 (t, *J* = 7.1 Hz, 3H), 0.96 (d, *J* = 6.7 Hz, 6H). ESI-MS: *m/z* 355.6[M+H] $^+$.

*4.1.8.2. Ethyl 2-[3-cyano-4-(2-methylallyloxy)phenyl]-6-imino-1,6-dihydropyrimidine-5-carboxylate (**18e**).* A white solid, yield: 93.9%. mp: 131.2 – 133.3°C. ^{1}H NMR (600 MHz, DMSO-d_6) δ 8.84 (s, 1H), 8.59 – 8.53 (m, 2H), 8.09 (s, 1H), 7.72 (s, 1H), 7.43 – 7.37 (m, 1H), 5.09 (d, 2H), 4.74 (s, 2H), 4.32 (q, *J* = 7.1 Hz, 2H), 1.82 (t, *J* = 1.2 Hz, 3H), 1.33 (t, *J* = 7.1 Hz, 3H). ESI-MS: *m/z* 339.4[M+H] $^+$.

*4.1.8.3. Ethyl 2-[4-(4-bromobenzyloxy)-3-cyanophenyl]-6-imino-1,6-dihydropyrimidine-5-carboxylate (**18j**).* A

white solid, yield: 72.3%。mp: 189.8 – 191.2°C. ^{1}H NMR (600 MHz, DMSO-d_6) δ 8.84 (s, 1H), 8.63 – 8.54 (m, 2H), 8.10 (s, 1H), 7.73 (s, 1H), 7.68 – 7.62 (m, 2H), 7.53 – 7.41 (m, 3H), 5.36 (s, 2H), 4.32 (q, *J* = 7.1 Hz, 2H), 1.33 (t, *J* = 7.1 Hz, 3H). ESI-MS: *m/z* 453.7[M+H] $^+$.

*4.1.8.4. Ethyl 2-[3-cyano-4-(4-methylbenzyloxy)phenyl]-6-imino-1,6-dihydropyrimidine-5-carboxylate (**18l**).* A white solid, yield: 86.5%. mp: 183.8 – 185.3°C. ^{1}H NMR (600 MHz, DMSO-d_6) δ 8.84 (s, 1H), 8.58 (d, *J* = 8.0 Hz, 2H), 8.10 (s, 1H), 7.72 (s, 1H), 7.52 (d, *J* = 1.6 Hz, 1H), 7.42 – 7.36 (m, 2H), 7.25 (d, *J* = 7.8 Hz, 2H), 5.32 (s, 2H), 4.32 (q, *J* = 7.1 Hz, 2H), 2.32 (s, 3H), 1.33 (t, *J* = 7.1 Hz, 3H). ESI-MS: *m/z* 389.4[M+H] $^+$.

*4.1.9. General procedure for synthesis of 2-(4-alkoxy-3-cyano)phenyl-6-oxo-1,6-dihydropyrimidine-5-carboxylic acids (**8a-l**) and 2-(4-alkoxy-3-cyano)phenyl-4-methyl-6-oxo-1,6-dihydropyrimidine-5-carboxylic acids (**9c, 9e, 9j, 9l**)*

A mixture of ethyl 2-(4-alkoxy-3-cyanophenyl)-6-oxo-1,6-dihydropyrimidine-5-carboxylate(**15a-l**) or ethyl 2-(4-alkoxy-3-cyanophenyl)-4-methyl-6-oxo-1,6-dihydropyrimidine-5-carboxylate(**16c**, **16e**, **16j**, **16l**) (1.1 mmol) , 10% LiOH aqueous (5 mL), EtOH (5 mL) and THF (5 mL) was stirred at 50°C for 2 h. The solvent was concentrated in a vacuum, and the residue was acidified with 1M hydrochloric acid to pH 1. The resulting precipitate was filtered, and refluxed for 0.5 h with a mixture of THF and H2O (2:1). Corresponding 2-(4-alkoxy-3-cyanophenyl)-4-methyl-6-oxo-1,6-dihydropyrimidine-5-carboxylic acids and

2-(4-alkoxy-3-cyano)phenyl-6-oxo-1,6-dihydropyrimidine-5-carboxylic acids were separated by filtration.

*4.1.9.1. 2-(3-Cyano-4-isopropoxyphenyl)-6-oxo-1,6-dihydropyrimidine-5-carboxylic acid (**8a**)*. A white solid, yield: 89.1%. mp: 238.5-240.8 °C. ^{1}H NMR (400 MHz, DMSO-d_6) δ 8.71 (s, 1H), 8.53 (d, *J* = 2.4 Hz, 1H), 8.45 (dd, *J* = 9.1, 2.4 Hz, 1H), 7.50 (d, *J* = 9.1 Hz, 1H), 4.96 (p, *J* = 6.0 Hz, 1H), and 1.37 (d, *J* = 6.0 Hz, 6H); ^{13}C NMR (100 MHz, DMSO) δ 166.97, 164.98, 162.84, 159.08, 156.47, 135.75, 134.82, 124.09, 116.03, 114.74, 111.95, 102.18, 72.88, and 21.97; ESI-HRMS: Calcd. for $C_{15}H_{13}N_3O_4$ [M–H]$^-$298.0906, found:298.0934; IR (KBr): *cm*$^{-1}$ 3432, 5154, 2244, 1732, 1643, 1556, 1290, 946.

*4.1.9.2. 2-(3-Cyano-4-isobutoxyphenyl)-6-oxo-1,6-dihydropyrimidine-5-carboxylic acid (**8b**)*. A white solid, yield: 82.1%. mp: 231.6-232.4°C; ^{1}H NMR (600 MHz, DMSO-d_6) δ 8.68 (d, *J* = 1.3 Hz, 1H), 8.54 (d, *J* = 2.3 Hz, 1H), 8.46 (dd, *J* = 9.1, 2.4 Hz, 1H), 7.45 (d, *J* = 9.1 Hz, 1H), 4.04 (d, *J* = 6.7 Hz, 2H), 2.10 (m, 1H), and 1.02 (d, *J* = 6.7 Hz, 6H); ^{13}C NMR (150 MHz, DMSO) δ 164.90, 164.44, 163.79, 163.55, 158.81, 135.88, 134.56, 124.09, 115.78, 114.03, 111.82, 101.59, 75.76, 28.01, and 19.14; ESI-HRMS: Calcd. for $C_{16}H_{15}N_3O_4$ [M–H]$^-$312.0990, found:312.0987; IR (KBr): *cm*$^{-1}$3406, 3071, 2230, 1709, 1645, 1566, 1291, 1009.

*4.1.9.3. 2-(3-Cyano-4-isopentyloxyphenyl)-6-oxo-1,6-dihydropyrimidine-5-carboxylic acid (**8c**)*. A white solid, yield: 83.2%. mp: 229.6-231.4 °C; ^{1}H NMR (600 MHz, DMSO-d_6) δ 8.71 (s, 1H), 8.52 (d, *J* = 2.4 Hz, 1H), 8.45 (dd, *J* = 9.0, 2.4 Hz, 1H), 7.48 (d, *J* = 9.1 Hz, 1H), 4.28 (t, *J* = 6.6 Hz,

2H), 1.82 (m, 1H), 1.69 (d, *J* = 6.6 Hz, 2H), and 0.96 (d, *J* = 6.6 Hz, 6H); ^{13}C NMR (100 MHz, DMSO) δ 166.92, 164.95, 163.67, 158.99, 156.43, 135.74, 134.50, 124.22, 115.83, 113.92, 111.88, 101.56, 68.66, 37.35, 25.09, and 22.81; ESI-HRMS: Calcd. for $C_{17}H_{17}N_3O_4$ $[M–H]^-$ 326.1146, found:326.1181; IR (KBr): *cm*$^{-1}$ 3462, 3079, 2233, 1709, 1643, 1564, 1291, 974.

*4.1.9.4. 2-(4-Allyloxy-3-cyanophenyl)-6-oxo-1,6-dihydropyrimidine-5-carboxylic acid (**8d**)*. A white solid, yield: 81.1%. mp: 226.2-229.5°C; ^{1}H NMR (400 MHz, DMSO-d_6) δ 8.71 (s, 1H), 8.55 (d, *J* = 2.4 Hz, 1H), 8.46 (dd, *J* = 9.0, 2.4 Hz, 1H), 7.46 (d, *J* = 9.0 Hz, 1H), 6.10 (m, 1H), 5.49 (m, 1H), 5.36 (m, 1H), and 4.88 (d, *J* = 5.2 Hz, 2H); ^{13}C NMR (100 MHz, DMSO) δ 166.99, 165.04, 163.15, 159.16, 156.47, 135.75, 134.63, 132.57, 124.77, 119.00, 115.89, 114.31, 112.02, 101.69, 70.24; ESI-HRMS: Calcd. for $C_{15}H_{11}N_3O_4$ $[M–H]^-$ 296.0677, found:296.0695; IR (KBr): *cm*$^{-1}$ 3462, 2081, 2234, 1706, 1644, 1566, 1297, 985.

*4.1.9.5. 2-[3-Cyano-4-(2-methylallyloxy)phenyl]-6-oxo-1,6-dihydropyrimidine-5-carboxylic acid (**8e**)*. A white solid, yield: 87.8%. mp: >250 °C; ^{1}H NMR (600 MHz, DMSO-d_6) δ 8.64 (s, 1H), 8.58 (d, *J* = 2.2 Hz, 1H), 8.53 (dd, *J* = 9.0, 2.3 Hz, 1H), 7.42 (d, J = 9.0 Hz, 1H), 5.13 (s, 1H), 5.03 (s, 1H), 4.76 (s, 2H), and 1.80 (s, 3H); ^{13}C NMR (100 MHz, DMSO) δ 170.21, 166.14, 162.84, 160.22, 155.22, 140.02, 135.50, 134.30, 126.56, 116.02, 114.21, 113.47, 110.74, 101.57, 72.66, and 19.44; ESI-HRMS: Calcd. for $C_{16}H_{13}N_3O_4$ $[M–H]^-$ 310.0833, found:310.0850; IR (KBr): *cm*$^{-1}$ 3451, 2232, 1626, 1563, 1300, 1004.

4.1.9.6.

2-[3-Cyano-4-(3-methylbut-2-en-1-yl)oxyphenyl]-6-oxo-1,6-dihydropyrimidine-5-carboxylic acid ***(8f)***. A white solid, yield:79.1%. mp: >250 °C; ^{1}H NMR (600 MHz, DMSO-d6) δ 8.73 (s, 1H), 8.54 (d, J = 2.4 Hz, 1H), 8.47 (dd, J = 9.0, 2.4 Hz, 1H), 7.49 (d, J = 9.1 Hz, 1H), 5.49 (t, J = 6.8 Hz, 1H), 4.84 (d, J = 6.8 Hz, 2H), and 1.78 (dd, J = 12.5, 1.3 Hz, 6H); ^{13}C NMR (100 MHz, DMSO) δ 164.97, 163.55, 159.11, 139.85, 135.74, 134.66, 124.33, 118.70, 116.01, 114.33, 112.06, 101.65, 66.90, 25.92, and 18.62; ESI-HRMS: Calcd. for $C_{17}H_{15}N_3O_4$ [M–H]$^-$324.0990, found:324.1007; IR (KBr): cm-1 3463, 3076, 2233, 1711, 1642, 1564, 1286, 969.

*4.1.9.7. 2-(4-Benzyloxy-3-cyanophenyl)-6-oxo-1,6-dihydropyrimidine-5-carboxylic acid (****8g****)*. White solid, yield: 83.9%. mp: >250 °C. ^{1}H NMR (600 MHz, DMSO-d6) δ 8.72 (s, 1H), 8.55 (d, J = 2.4 Hz, 1H), 8.46 (dd, J = 9.0, 2.4 Hz, 1H), 7.57 (d, J = 9.1 Hz, 1H), 7.51 (d, J = 7.0 Hz, 2H), 7.44 (t, J = 7.5 Hz, 2H), 7.41 – 7.35 (m, 1H), and 5.41 (s, 2H); ^{13}C NMR (100 MHz, DMSO) δ 166.68, 164.96, 163.31, 159.09, 156.67, 135.91, 135.80, 134.68, 129.10, 128.83, 128.19, 124.75, 115.90, 114.49, 112.17, 101.88, and 71.31; ESI-HRMS: Calcd. for $C_{19}H_{13}N_3O_4$ [M–H]$^-$346.0833, found:346.0822; IR (KBr): *cm^{-1}* 3461, 3076, 2231, 1699, 1632, 1564, 1290, 1013.

4.1.9.8. 2-[3-Cyano-4-(4-fluorobenzyloxy)phenyl]-6-oxo-1,6-dihydropyrimidine-5-carboxylic acid ***(8h)***. A white solid, yield: 81.9%, mp: >250 °C; ^{1}H NMR (600 MHz, DMSO-d6) δ 8.72 (s, 1H), 8.57 (d, J = 2.4 Hz, 1H), 8.49 (dd, J = 9.0, 2.4 Hz, 1H), 7.57 (td, J = 6.4, 1.6 Hz, 3H), 7.29 (t, J = 8.9 Hz, 2H), and 5.39 (s, 2H); ^{13}C NMR (100 MHz, DMSO) δ 165.32, 163.73, 163.08, 161.31, 159.56, 135.77, 134.61, 132.23, 130.67, 130.59, 125.48, 116.10, 115.95, 115.88, 114.47, 101.81, and 70.59; ESI-HRMS: Calcd. for $C_{19}H_{12}FN_3O_4$ [M–H]$^-$364.0739, found:364.0731; IR (KBr): *cm^{-1}*

3452,3080,2233,1698,1632,1565,1299,1011.

4.1.9.9. 2-[4-(4-Chlorobenzyloxy)-3-cyanophenyl]-6-oxo-1,6-dihydropyrimidine-5-carboxylic acid ***(8i)***. A white solid, yield: 89.1%. mp: >250 °C. ^{1}H NMR (600 MHz, DMSO-d_6) δ 8.71 (s, 1H), 8.58 (s, 1H), 8.52 – 8.46 (m, 1H), 7.66 – 7.42 (m, 5H), and 5.41 (s, 2H); ^{13}C NMR (100 MHz, DMSO) δ 169.06, 165.89, 162.82, 160.13, 156.06, 135.66, 135.09, 134.49, 133.46, 130.09, 129.16, 126.49, 116.04, 114.40, 111.33, 101.78, and 70.41; ESI-HRMS: Calcd. for $C_{19}H_{12}ClN_3O_4$ [M–H]$^-$380.0444, found:380.0420; IR (KBr): *cm*$^{-1}$ 3460, 3086, 2230, 1696, 1631, 1565, 1295, 1012.

4.1.9.10. 2-[4-(4-Bromobenzyloxy)-3-cyanophenyl]-6-oxo-1,6-dihydropyrimidine-5-carboxylic acid ***(8j)***. A white solid, yield: 90.1%. mp: >250 °C. ^{1}H NMR (600 MHz, DMSO-d_6) δ 8.73 (s, 1H), 8.57 (d, *J* = 2.4 Hz, 1H), 8.48 (dd, *J* = 9.0, 2.4 Hz, 1H), 7.72 – 7.62 (m, 2H), 7.56 (d, *J* = 9.1 Hz, 1H), 7.51 – 7.41 (m, 2H), and 5.40 (s, 2H); ^{13}C NMR (100 MHz, DMSO) δ 166.90, 165.32, 164.67, 162.89, 161.15, 137.35, 136.20, 133.81, 132.26, 132.17, 127.06, 117.69, 117.54, 117.47, 116.05, 103.40, 72.18; ESI-HRMS: Calcd. for $C_{19}H_{12}BrN_3O_4$ [M–H]$^-$423.9938, found:423.9913; IR (KBr): *cm*$^{-1}$ 3461, 3079, 2229, 1700, 1631, 1565, 1295, 1009.

4.1.9.11. 2-[4-(4-tert-Butylbenzyloxy)-3-cyanophenyl]-6-oxo-1,6-dihydropyrimidine-5-carboxylic acid ***(8k)***. A white solid, yield: 90.9%. mp: >250 °C. ^{1}H-NMR (400 MHz, DMSO-d6) δ 8.72 (s, 1H), 8.64 – 8.51 (m, 2H), 7.60 – 7.17 (m, 5H), 5.27 (s, 2H), and 1.29 (s, 9H); ^{13}C-NMR (100 MHz, DMSO) δ 173.66, 172.09, 162.19, 161.13, 159.83, 151.17, 134.63, 133.37, 128.12, 125.79, 116.99, 115.93, 113.50, 100.83, 70.65, 34.79, and 31.56; ESI-HRMS: Calcd. for $C_{23}H_{21}N_3O_4$ [M–

H]$^-$402.1459, found:402.1466; IR (KBr): *cm*$^{-1}$ 3453, 2962, 2231, 1605, 1476, 1282, 1007.

*4.1.9.12. 2-[3-Cyano-4-(4-methylbenzyloxy)phenyl]-6-oxo-1,6-dihydropyrimidine-5-carboxylic acid (**8l**)*. A white solid, yield: 89.9%. mp: >250 °C. ^{1}H NMR (400 MHz, DMSO-d_6) δ 8.72 (s, 1H), 8.56 (s, 1H), 8.47 (d, *J* = 9.1 Hz, 1H), 7.57 (d, *J* = 9.1 Hz, 1H), 7.39 (d, *J* = 7.8 Hz, 2H), 7.25 (d, *J* = 8.1 Hz, 2H), 5.37 (s, 2H), and 2.32 (s, 3H); ^{13}C NMR (100 MHz, DMSO) δ 169.02, 165.87, 162.80, 160.11, 156.02, 135.64, 135.06, 134.47, 133.44, 130.06, 129.13, 126.46, 116.02, 114.38, 111.31, 101.76, 70.39, and 25.59; ESI-HRMS: Calcd. for $C_{20}H_{15}N_3O_4$ [M–H]$^-$360.0990, found:360.0969; IR (KBr): *cm*$^{-1}$ 3423, 3075, 2229, 1702, 1631, 1563, 1298, 1015.

*4.1.9.13. 2-(3-Cyano-4-isopentyloxyphenyl)-4-methyl-6-oxo-1,6-dihydropyrimidine-5-carboxylic acid (**9c**)*. A white solid, yield: 96.1%. mp: >250 °C. ^{1}H NMR (600 MHz, DMSO-d_6) δ 8.53 (d, *J* = 2.4 Hz, 1H), 8.45 (dd, *J* = 9.0, 2.4 Hz, 1H), 7.49 (d, *J* = 9.0 Hz, 1H), 4.29 (t, *J* = 6.6 Hz, 2H), 2.65 (s, 3H), 1.83 (m, 1H), 1.70 (q, *J* = 6.6 Hz, 2H), and 0.97 (d, *J* = 6.6 Hz, 6H); ^{13}C NMR (100 MHz, DMSO) δ 166.80, 166.18, 163.44, 158.27, 156.13, 135.75, 134.49, 124.68, 115.99, 113.85, 110.83, 101.40, 68.59, 37.37, 25.09, 23.10, and 22.83; ESI-HRMS: Calcd. for $C_{18}H_{19}N_3O_4$ [M–H]$^-$ 340.1376, found:340.1352; IR (KBr): *cm*$^{-1}$ 3454, 2956, 2229, 1737, 1608, 1554, 1298, 992.

4.1.9.14.

*2-[3-Cyano-4-(2-methylallyloxy)phenyl]-4-methyl-6-oxo-1,6-dihydropyrimidine-5-carboxylic acid (**9e**)*. A white solid, yield: 91.1%. mp: >250 □. ^{1}H NMR (600 MHz, DMSO-d_6) δ 8.55 (d, *J* = 2.4 Hz, 1H), 8.43 (dd, *J* = 9.0, 2.4 Hz, 1H), 7.46 (d, *J* = 9.1 Hz, 1H), 5.14 (s, 1H), 5.07 – 5.02 (m, 1H), 4.79

(s, 2H), 2.65 (s, 3H), 1.82 (s, 3H). ^{13}C NMR (100 MHz, DMSO) δ 165.94, 163.08, 162.67, 162.35, 155.73, 139.96, 135.70, 134.56, 124.54, 115.89, 114.29, 113.56, 101.63, 72.74, 19.44. ESI-HRMS: Calcd. for $C_{17}H_{15}N_3O_4$ $[M–H]^-$324.1063, found:324.1030. IR (KBr): *cm*$^{-1}$ 3443, 2924, 2229, 1706, 1613, 1569, 1287, 998.

4.1.9.15.

*2-[4-(4-Bromobenzyloxy)-3-cyanophenyl]-4-methyl-6-oxo-1,6-dihydropyrimidine-5-carboxylic acid (**9j**)*. A white solid, yield: 94.1%. mp: >250 □. ^{1}H NMR (600 MHz, DMSO-d_6) δ 8.55 (d, *J* = 2.4 Hz, 1H), 8.44 (dd, *J* = 9.0, 2.4 Hz, 1H), 7.66 (dd, *J* = 8.5, 2.8 Hz, 2H), 7.54 (d, *J* = 9.2 Hz, 1H), 7.47 (d, *J* = 8.1 Hz, 2H), 5.39 (s, 2H), 2.51 (s, 3H). ^{13}C NMR (100 MHz, DMSO) δ 166.63, 165.93, 162.77, 160.83, 157.61, 135.61, 135.29, 134.49, 131.94, 130.22, 121.91, 115.80, 114.27, 101.64, 70.34, 26.11. ESI-HRMS: Calcd. for $C_{20}H_{14}BrN_3O_4$ $[M–H]^-$438.0095, found:438.0064. IR (KBr): *cm*$^{-1}$ 3437, 2921, 2229, 1717, 1609, 1502, 1285, 1119.

4.1.9.16.

*2-[3-Cyano-4-(4-methylbenzyloxy)phenyl]-4-methyl-6-oxo-1,6-dihydropyrimidine-5-carboxylic acid (**9l**)*. A white solid, yield: 89.9%. mp: >250 ℃. ^{1}H-NMR (400 MHz, DMSO-d_6) δ 8.54 (d, *J* = 2.3 Hz, 1H), 8.44 (dd, *J* = 9.0, 2.4 Hz, 1H), 7.55 (d, *J* = 9.1 Hz, 1H), 7.39 (d, *J* = 8.1 Hz, 2H), 7.24 (d, *J* = 8.0 Hz, 2H), 5.36 (s, 2H), 2.65 (s, 3H), 2.32 (s, 3H). ^{13}C-NMR (100 MHz, DMSO) δ 165.97, 164.91, 163.19, 155.95, 138.20, 135.87, 134.82, 132.89, 129.64, 128.39, 124.52, 115.97, 114.39, 101.69, 71.25, 21.27. ESI-HRMS: Calcd. for $C_{21}H_{17}N_3O_4$ $[M–H]^-$374.1146, found:374.1159. IR (KBr): *cm*$^{-1}$ 3435, 2922, 2231, 1706, 1606, 1502, 1291, 1117.

4.1.10. General procedure for synthesis of 2-(4-alkoxy-3-cyano)phenyl-6-imino-1,6-dihydropyrimidine-5-carboxylic acids (**10c, 10e, 10j, 10l**)

A mixture of ethyl 2-(4-alkoxy-3-cyanophenyl)-6-amino-1,6-dihydropyrimidine-5-carboxylate (1.1 mmol), 10% LiOH aqueous (5 mL), EtOH (5 mL) and THF (5 mL) was stirred at 50°C for 2h. The solvent was concentrated in a vacuum, and the residue was acidified with acetic acid to pH 3-4. The resulting precipitate was filtered, and refluxed for 0.5 h with a mixture of THF and H_2O (2:1). Corresponding 2-(4-alkoxy-3-cyano)phenyl-6-imino-1,6-dihydropyrimidine-5-carboxylic acids were separated by filtration.

*4.1.10.1. 2-(3-Cyano-4-isopentyloxyphenyl)-6-imino-1,6-dihydropyrimidine-5-carboxylic acid (**10c**)*. A white solid, yield: 83.1%. mp: >250 °C. ^{1}H NMR (600 MHz, DMSO-d_6) δ 8.80 (s, 1H), 8.65 – 8.48 (m, 2H), 8.24 (s, 1H), 7.98 (s, 1H), 7.44 (d, J = 8.8 Hz, 1H), 4.26 (t, J = 6.7 Hz, 2H), 1.83 (m, 1H), 1.70 (q, J = 6.7 Hz, 2H), and 0.96 (d, J = 6.7 Hz, 6H); ^{13}C NMR (150 MHz, DMSO) δ 167.64, 163.06, 162.88, 162.82, 158.75, 135.26, 133.96, 129.28, 116.39, 113.72, 103.50, 101.28, 68.34, 37.43, 25.09, and 22.86; ESI-HRMS: Calcd. for $C_{17}H_{18}N_4O_3$ [M+H] $^-$ 325.1306, found:325.1310; IR (KBr): *cm^{-1}* 3428, 2957, 2229, 1605, 1387, 1286, 1149, 975.

*4.1.10.2. 2-[3-Cyano-4-(2-methylallyloxy)phenyl]-6-imino-1,6-dihydropyrimidine-5-carboxylic acid (**10e**)*. A white solid, yield: 79.2%. mp: >250 °C. ^{1}H NMR (600 MHz, DMSO-d_6) δ 8.76 (s, 1H), 8.71 – 8.49 (m, 3H), 8.24 (s, 1H), 7.46 (d, J = 9.0 Hz, 1H), 5.14 (s, 1H), 5.04 (s, 1H), 4.77 (s, 2H), and 1.82 (s, 3H); ^{13}C NMR (150 MHz, DMSO) δ 165.99, 161.93, 161.70, 160.19, 155.33, 139.03,

138.98, 134.26, 133.13, 115.10, 113.17, 112.43, 102.67, 100.51, 71.58, and 18.41; ESI-HRMS: Calcd. for $C_{16}H_{14}N_4O_3$ $[M–H]^-$309.0993, found:309.0989; IR (KBr): cm^{-1} 3428, 2957, 2229, 1605, 1387, 1286, 1149, 975.

*4.1.10.3. 2-[4-(4-Bromobenzyloxy)-3-cyanophenyl]-6-imino-1,6-dihydropyrimidine-5-carboxylic acid (**10j**)*. A white solid, yield: 77.3%. mp: >250 °C. ^{1}H NMR (400 MHz, DMSO-d_6) δ 8.80 – 8.75 (m, 1H), 8.67 – 8.46 (m, 3H), 8.21 (s, 1H), 7.65 (d, J = 8.4 Hz, 2H), 7.55 (d, J = 8.9 Hz, 1H), 7.48 (d, J = 8.4 Hz, 2H), and 5.38 (s, 2H); ^{13}C NMR (100 MHz, DMSO) δ 166.79, 162.99, 162.79, 135.46, 134.40, 132.05, 130.37, 122.02, 116.11, 114.43, 103.87, 101.81, and 70.44; ESI-HRMS: Calcd. for $C_{19}H_{13}BrN_4O_3$ $[M–H]^-$423.0098, found:423.0063; IR (KBr): cm^{-1} 3374, 2918, 2235, 1604, 1347, 1287, 1151, 1007.

*4.1.10.4. 2-[3-Cyano-4-(4-methylbenzyloxy)phenyl]-6-imino-1,6-dihydropyrimidine-5-carboxylic acid (**10l**)*. A white solid, yield: 80.0%. mp: >250 °C. ^{1}H NMR (600 MHz, DMSO-d_6) δ 8.79 (s, 1H), 8.58 (d, J = 8.4 Hz, 2H), 8.41 (s, 1H), 8.10 (s, 1H), 7.55 (d, J = 8.9 Hz, 1H), 7.40 (d, J = 7.7 Hz, 2H), 7.25 (d, J = 7.7 Hz, 2H), 5.33 (s, 2H), and 2.32 (s, 3H); ^{13}C NMR (100 MHz, DMSO) δ 167.21, 163.02, 162.79, 157.05, 138.17, 135.28, 134.19, 132.99, 129.63, 128.40, 116.28, 114.34, 103.69, 101.69, 71.15, and 21.27; ESI-HRMS: Calcd. for $C_{20}H_{16}N_4O_3$ $[M–H]^-$359.1150, found:359.1124; IR (KBr): cm^{-1} 3429, 2957, 2230, 1603, 1385, 1285, 1142, 997.

4.2. Assay of the in vitro XO inhibitory activity

The XO activity with xanthine as the substrate was assayed spectrophotometrically by

measuring uric acid formation at 295 nm at 25 °C according to the procedure reported by Zhang *et al*. [11] with modification. XO (Sigma, X4875) was diluted with a buffer (0.1 M sodium pyrophosphate and 0.3 mM Na_2EDTA, pH 8.3) to make the enzyme solution (75 U/L). Xanthine (J&K) was dissolved and diluted with the buffer to obtain the substrate solution (500 μM). The tested compounds were initially dissolved in DMSO to yield a 10000 nM solution, which was then further diluted with buffer to obtain the required concentrations. The buffer (67 μL), enzyme solution (75 U/L, 40 μL) and sample (53 μL) or blank solution (buffer) were added to 96-well plates (COSTAR 3599) and incubated at 25 °C for 15 min. Then, the substrate solution (40 μL) was added to the plates with a total volume of 200 μL, which was further scanned to measure the absorbance change immediately at 295 nm and at 30 s intervals for 2 min. Febuxostat and allopurinol were used as positive controls. All the tests were performed in triplicate. Compounds presenting inhibitory effects over 50% at a concentration of 10 μM were further tested at a wide range of concentrations to calculate their IC_{50} value by using SPSS 20.0 software (SPSS Inc, IL, USA).

Enzyme kinetic assays were performed in the same way as the XO assay but with varying concentrations of substrate solution at 400, 500, 600 and 700 μM (final concentrations of the substrate were 80, 100, 120 and 140 μM, respectively).

4.3. Molecular modeling

Molecular docking studies were performed using GLIDE (2016, Schrodinger Suite). The crystal structure of XO in a complex with febuxostat (PDB code: 1N5X) obtained from the Protein Data Bank was adopted in docking calculations. All bound water was eliminated from the protein, and all hydrogen atoms were added to the proteins. The protein was prepared, optimized and minimized by

Protein Preparation Wizard (2016, Schrodinger Suite) using an OPLS-2005 force field. The ligands were built within Maestro BUILD (2016, Schrodinger Suite) and prepared by the LIGPREP module. The tautomeric forms of ligands, which include the keto and enol forms of ligands, were generated at physiological pH (7.0 ± 2.0 pH). The active site for docking was defined as a grid box of dimensions 25×25×25 $Å^3$ around the centroid of the ligand assuming that the ligands to be docked were of a size similar to the co-crystallized ligand. The docking methodology has been validated by extracting the crystallographic bound febuxostat and redocking it with the Glide module using extra precision (XP) to the catalytic site of 1N5X. This validation provided a root mean square deviation (rmsd) of 0.046 Å between the docked versus the experimental conformation. Different docking poses of ligands were generated and analyzed for interpretation of the final results. Accelrys Discovery Studio Visualizer 2017 [49] was used for graphical display.

4.4 In vivo hypouricemic effect assay

Male Sprague-Dawley rats (6 weeks old, n = 8) were purchased from the Animal Center of Shenyang Pharmaceutical University (Shenyang, China). Number of Approval of Ethics Committee: SYPU-IACUC-2019-1-11-203. Animal maintenance and treatment met the protocols approved by the Ethics Review Committee for Animal Experimentation of Shenyang Pharmaceutical University. The rats had free access to food and water and were maintained on a 12-h light/dark cycle in a temperature- and humidity-controlled room for a week.

After fasting for 12 h with free access to water prior to the experiment, rats were randomly divided into five groups and intragastrically administered febuxostat (5 mg/kg), allopurinol (10 mg/kg) and the test compound **10c** (5 mg/kg) dissolved in a 0.5% CMC-Na solution, respectively, whereas the other two groups were treated with 0.5% CMC-Na. Febuxostat and allopurinol were used as the positive control drugs. Then, rats not in the blank group were injected intraperitoneally with potassium oxonate (300 mg/kg) 1 h after drug administration to increase the serum urate level [50]. Blood samples were collected from the rats via orbital vein bleeding at 2, 3, 4, 6 and 8 h after drug administration. The collected blood samples were allowed to clot at room temperature for 2 h,

followed by centrifuging at 3000 g at 4 °C for 10 min. The sUA levels were determined with a uric acid assay kit (Nanjing Jiancheng Bioengineering Institute, China) in accordance with the manufacturer's instructions.

The statistical analysis was performed using Student's *t*-test to determine the level of significance. Data are presented as the means ± SDs. The figures were obtained with the GraphPad 6.0 (GraphPad Software, Inc., San Diego, CA) statistical system.

4.5 Acute oral toxicity study

Healthy KM mice (18-22 g) were purchased from the Animal Center of Shenyang Pharmaceutical University (Shenyang, China). Number of Approval of Ethics Committee: SYPU-IACUC-2019- 6-26-106. Animal maintenance and treatment met the protocols approved by the Ethics Review Committee for Animal Experimentation of Shenyang Pharmaceutical University. The rats had free access to food and water and were maintained on a 12-h light/dark cycle in a temperature- and humidity-controlled room for a week.

After fasting for 4 h with free access to water prior to the experiment, two groups of mice each consisting of 3 male mice and 3 female mice were employed for acute toxicity studies for compound **10c**. The test compound **10c** (2000 mg/kg) was dissolved in a 0.5% CMC-Na solution. The first group was treated with 0.5% CMC-Na and served as the vehicle control. The other group was treated with a single higher oral dose (2000 mg/kg) of compound **10c**. The mice were observed continuously for any signs and symptoms of toxicity for 24 h after treatment.

Acknowledgments

This work was supported by National Natural Science Foundation of China (Grant No.81773813). Specially, we are grateful to professor Zheng Liu and his team for their support on the *in vivo* hypouricemic effect assay.

References

[1] G. Luna, A.V. Dolzhenko, R.L. Mancera, Inhibitors of Xanthine Oxidase: Scaffold Diversity and Structure-Based Drug Design, ChemMedChem, 14 (2019) 714-743.
[2] P.C. Robinson, Gout - An update of aetiology, genetics, co-morbidities and management, Maturitas, 118 (2018) 67-73.
[3] F. Rees, M. Hui, M. Doherty, Optimizing current treatment of gout, Nat Rev Rheumatol, 10 (2014) 271-283.
[4] R. Kumar, G. Joshi, H. Kler, S. Kalra, M. Kaur, R. Arya, Toward an Understanding of Structural Insights of Xanthine and Aldehyde Oxidases: An Overview of their Inhibitors and Role in Various Diseases, Med Res Rev, 38 (2018) 1073-1125.
[5] R. Kumar, Darpan, S. Sharma, R. Singh, Xanthine oxidase inhibitors: a patent survey, Expert Opin Ther Pat, 21 (2011) 1071-1108.
[6] R. Ojha, J. Singh, A. Ojha, H. Singh, S. Sharma, K. Nepali, An updated patent review: xanthine oxidase inhibitors for the treatment of hyperuricemia and gout (2011-2015), Expert Opin Ther Pat, 27 (2017) 311-345.
[7] C. Chen, J.-M. Lü, Q. Yao, Hyperuricemia-Related Diseases and Xanthine Oxidoreductase (XOR) Inhibitors: An Overview, Medical Science Monitor, 22 (2016) 2501-2512.
[8] A. Fais, B. Era, S. Asthana, V. Sogos, R. Medda, L. Santana, E. Uriarte, M.J. Matos, F. Delogu, A. Kumar, Coumarin derivatives as promising xanthine oxidase inhibitors, Int J Biol Macromol, 120 (2018) 1286-1293.
[9] A. Fukunari, K. Okamoto, T. Nishino, B.T. Eger, E.F. Pai, M. Kamezawa, I. Yamada, N. Kato, Y-700 [1-[3-Cyano-4-(2,2-dimethylpropoxy)phenyl]-1H-pyrazole-4-carboxylic acid]: a potent xanthine oxidoreductase inhibitor with hepatic excretion, J Pharmacol Exp Ther, 311 (2004) 519-528.
[10] J. Li, F. Wu, X. Liu, Y. Zou, H. Chen, Z. Li, L. Zhang, Synthesis and bioevaluation of 1-phenyl-pyrazole-4-carboxylic acid derivatives as potent xanthine oxidoreductase inhibitors, Eur J Med Chem, 140 (2017) 20-30.
[11] Q. Guan, Z. Cheng, X. Ma, L. Wang, D. Feng, Y. Cui, K. Bao, L. Wu, W. Zhang, Synthesis and bioevaluation of 2-phenyl-4-methyl-1,3-selenazole-5-carboxylic acids as potent xanthine

oxidase inhibitors, Eur J Med Chem, 85 (2014) 508-516.
[12] S. Wang, J. Yan, J. Wang, J. Chen, T. Zhang, Y. Zhao, M. Xue, Synthesis of some 5-phenylisoxazole-3-carboxylic acid derivatives as potent xanthine oxidase inhibitors, Eur J Med Chem, 45 (2010) 2663-2670.
[13] S. Chen, T. Zhang, J. Wang, F. Wang, H. Niu, C. Wu, S. Wang, Synthesis and evaluation of 1-hydroxy/methoxy-4-methyl-2-phenyl-1H-imidazole-5-carboxylic acid derivatives as non-purine xanthine oxidase inhibitors, Eur J Med Chem, 103 (2015) 343-353.
[14] A. Shi, D. Wang, H. Wang, Y. Wu, H. Tian, Q. Guan, K. Bao, W. Zhang, Synthesis and bioevaluation of 2-phenyl-5-methyl-2H-1,2,3-triazole-4-carboxylic acid/carbohydrazide derivatives as potent xanthine oxidase inhibitors, RSC Advances, 6 (2016) 114879-114888.
[15] T.J. Zhang, Q.X. Wu, S.Y. Li, L. Wang, Q. Sun, Y. Zhang, F.H. Meng, H. Gao, Synthesis and evaluation of 1-phenyl-1H-1,2,3-triazole-4-carboxylic acid derivatives as xanthine oxidase inhibitors, Bioorganic & medicinal chemistry letters, 27 (2017) 3812-3816.
[16] J.U. Song, S.P. Choi, T.H. Kim, C.K. Jung, J.Y. Lee, S.H. Jung, G.T. Kim, Design and synthesis of novel 2-(indol-5-yl)thiazole derivatives as xanthine oxidase inhibitors, Bioorganic & medicinal chemistry letters, 25 (2015) 1254-1258.
[17] J.U. Song, J.W. Jang, T.H. Kim, H. Park, W.S. Park, S.H. Jung, G.T. Kim, Structure-based design and biological evaluation of novel 2-(indol-2-yl) thiazole derivatives as xanthine oxidase inhibitors, Bioorg Med Chem Lett, 26 (2016) 950-954.
[18] A. Mehmood, M. Ishaq, L. Zhao, B. Safdar, A.U. Rehman, M. Munir, A. Raza, M. Nadeem, W. Iqbal, C. Wang, Natural compounds with xanthine oxidase inhibitory activity: A review, Chem Biol Drug Des, 93 (2019) 387-418.
[19] R. Dhiman, S. Sharma, G. Singh, K. Nepali, P.M. Singh Bedi, Design and Synthesis of Aza-Flavones as a New Class of Xanthine Oxidase Inhibitors, Archiv der Pharmazie, 346 (2013) 7-16.
[20] S. Sharma, K. Sharma, R. Ojha, D. Kumar, G. Singh, K. Nepali, P.M. Bedi, Microwave assisted synthesis of naphthopyrans catalysed by silica supported fluoroboric acid as a new class of non purine xanthine oxidase inhibitors, Bioorg Med Chem Lett, 24 (2014) 495-500.
[21] H. Singh, S. Sharma, R. Ojha, M.K. Gupta, K. Nepali, P.M. Bedi, Synthesis and evaluation of naphthoflavones as a new class of non purine xanthine oxidase inhibitors, Bioorg Med Chem Lett, 24 (2014) 4192-4197.
[22] M. Kaur, A. Kaur, S. Mankotia, H. Singh, A. Singh, J.V. Singh, M.K. Gupta, S. Sharma, K. Nepali, P.M.S. Bedi, Synthesis, screening and docking of fused pyrano[3,2-d]pyrimidine derivatives as xanthine oxidase inhibitor, Eur J Med Chem, 131 (2017) 14-28.
[23] H.S. Virdi, S. Sharma, S. Mehndiratta, P.M.S. Bedi, K. Nepali, Design, synthesis and evaluation of 2,4-diarylpyrano[3,2-c]chromen-5(4H)-one as a new class of non-purine xanthine oxidase inhibitors, Journal of Enzyme Inhibition and Medicinal Chemistry, 30 (2015) 730-736.
[24] J.V. Singh, G. Mal, G. Kaur, M.K. Gupta, A. Singh, K. Nepali, H. Singh, S. Sharma, P.M. S. Bedi, Benzoflavone derivatives as potent antihyperuricemic agents, MedChemComm, 10 (2019) 128-147.
[25] R. Kaur, F. Naaz, S. Sharma, S. Mehndiratta, M.K. Gupta, P.M.S. Bedi, K. Nepali, Screening of a library of 4-aryl/heteroaryl-4H-fused pyrans for xanthine oxidase inhibition: synthesis, biological evaluation and docking studies, Medicinal Chemistry Research, 24 (2015) 3334-3349.

[26] C.M. Burns, R.L. Wortmann, Gout therapeutics: new drugs for an old disease, The Lancet, 377 (2011) 165-177.

[27] K. Matsumoto, K. Okamoto, N. Ashizawa, T. Nishino, FYX-051: A Novel and Potent Hybrid-Type Inhibitor of Xanthine Oxidoreductase, Journal of Pharmacology and Experimental Therapeutics, 336 (2010) 95-103.

[28] H. Choi, T. Neogi, L. Stamp, N. Dalbeth, R. Terkeltaub, New Perspectives in Rheumatology: Implications of the Cardiovascular Safety of Febuxostat and Allopurinol in Patients With Gout and Cardiovascular Morbidities Trial and the Associated Food and Drug Administration Public Safety Alert, Arthritis Rheumatol, 70 (2018) 1702-1709.

[29] FDA adds Boxed Warning for increased risk of death with gout medicine Uloric (febuxostat) https://www.fda.gov/drugs/drug-safety-and-availability/fda-adds-boxed-warning-increased-risk-death-gout-medicine-uloric-febuxostat

[30] A. Smelcerovic, K. Tomovic, Z. Smelcerovic, Z. Petronijevic, G. Kocic, T. Tomasic, Z. Jakopin, M. Anderluh, Xanthine oxidase inhibitors beyond allopurinol and febuxostat; an overview and selection of potential leads based on in silico calculated physico-chemical properties, predicted pharmacokinetics and toxicity, Eur J Med Chem, 135 (2017) 491-516.

[31] G. Sandmann, Bleaching Activities of Substituted Pyrimidines and Structure-Activity Comparison to Related Heterocyclic Derivatives, Pesticide Biochemistry and Physiology, 70 (2001) 86-91.

[32] J. Haque, K.R. Ansari, V. Srivastava, M.A. Quraishi, I.B. Obot, Pyrimidine derivatives as novel acidizing corrosion inhibitors for N80 steel useful for petroleum industry: A combined experimental and theoretical approach, Journal of Industrial and Engineering Chemistry, 49 (2017) 176-188.

[33] J.B. Shi, W.J. Tang, X.B. Qi, R. Li, X.H. Liu, Novel pyrazole-5-carboxamide and pyrazole-pyrimidine derivatives: synthesis and anticancer activity, Eur J Med Chem, 90 (2015) 889-896.

[34] B.R. C, A. Kulkarni-Almeida, K.V. Katkar, S. Khanna, U. Ghosh, A. Keche, P. Shah, A. Srivastava, V. Korde, K.V. Nemmani, N.J. Deshmukh, A. Dixit, M.K. Brahma, U. Bahirat, L. Doshi, R. Sharma, H. Sivaramakrishnan, Identification of novel isocytosine derivatives as xanthine oxidase inhibitors from a set of virtual screening hits, Bioorg Med Chem, 20 (2012) 2930-2939.

[35] S. Khanna, S. Burudkar, K. Bajaj, P. Shah, A. Keche, U. Ghosh, A. Desai, A. Srivastava, A. Kulkarni-Almeida, N.J. Deshmukh, A. Dixit, M.K. Brahma, U. Bahirat, L. Doshi, K.V. Nemmani, P. Tannu, A. Damre, B.R. C, R. Sharma, H. Sivaramakrishnan, Isocytosine-based inhibitors of xanthine oxidase: design, synthesis, SAR, PK and in vivo efficacy in rat model of hyperuricemia, Bioorg Med Chem Lett, 22 (2012) 7543-7546.

[36] K. Bajaj, S. Burudkar, P. Shah, A. Keche, U. Ghosh, P. Tannu, S. Khanna, A. Srivastava, N.J. Deshmukh, A. Dixit, Y. Ahire, A. Damre, K.V. Nemmani, A. Kulkarni-Almeida, B.R. C, R. Sharma, H. Sivaramakrishnan, Lead optimization of isocytosine-derived xanthine oxidase inhibitors, Bioorg Med Chem Lett, 23 (2013) 834-838.

[37] J. Evenas, F. Edfeldt, M. Lepisto, N. Svitacheva, A. Synnergren, B. Lundquist, M. Granse, A. Ronnholm, M. Varga, J. Wright, M. Wei, S. Yue, J. Wang, C. Li, X. Li, G. Chen, Y. Liao, G. Lv, A. Tjornebo, F. Narjes, HTS followed by NMR based counterscreening. Discovery and optimization

of pyrimidones as reversible and competitive inhibitors of xanthine oxidase, Bioorg Med Chem Lett, 24 (2014) 1315-1321.

[38] Y. Yamaguchi, T. Matsumura, K. Ichida, K. Okamoto, T. Nishino, Human xanthine oxidase changes its substrate specificity to aldehyde oxidase type upon mutation of amino acid residues in the active site: roles of active site residues in binding and activation of purine substrate, J Biochem, 141 (2007) 513-524.

[39] B. Damle, M.V. Varma, N. Wood, Pharmacokinetics of voriconazole administered concomitantly with fluconazole and population-based simulation for sequential use, Antimicrob Agents Chemother, 55 (2011) 5172-5177.

[40] M. Schachter, Chemical, pharmacokinetic and pharmacodynamic properties of statins: an update, Fundam Clin Pharmacol, 19 (2005) 117-125.

[41] OECD Guidelines for the Testing of Chemicals, ed. OECD, OECD Publishing, Paris, France, 2001, pp. 1–14.

[42] A.V. Laptev, A.Y. Lukin, N.E. Belikov, K.V. Zvezdin, O.V. Demina, V.A. Barachevsky, S.D. Varfolomeev, A.A. Khodonov, V.I. Shvets, Synthesis and studies of photochromic properties of spirobenzopyran carboxy derivatives and their model compounds as potential markers, Russian Chemical Bulletin, 63 (2015) 2026-2035.

[43] A.K. Chakraborti, G Kaur, One-pot synthesis of nitriles from aldehydes under microwave irradiation: influence of the medium and mode of microwave irradiation on product formation, Tetrahedron, 55(1999) 13265-13268.

[44] X Lu, X Xin, B Wan, Silver-catalyzed [3+ 2+ 1] annulation of aryl amidines with benzyl isocyanide, Tetrahedron Letters, 59(2018) 361-364.

[45] T. Goto, A. Shiina, T. Yoshino, K. Mizukami, K. Hirahara, O. Suzuki, Y. Sogawa, T. Takahashi, T. Mikkaichi, N. Nakao, M. Takahashi, M. Hasegawa, S. Sasaki, Synthesis and biological evaluation of 5-carbamoyl-2-phenylpyrimidine derivatives as novel and potent PDE4 inhibitors, Bioorg Med Chem, 21 (2013) 7025-7037.

[46] E.J. Barreiro, A.E. Kummerle, C.A. Fraga, The methylation effect in medicinal chemistry, Chem Rev, 111 (2011) 5215-5246.

[47] Z. Xie, X. Luo, Z. Zou, X. Zhang, F. Huang, R. Li, S. Liao, Y. Liu, Synthesis and evaluation of hydroxychalcones as multifunctional non-purine xanthine oxidase inhibitors for the treatment of hyperuricemia, Bioorganic & medicinal chemistry letters, 27 (2017) 3602-3606.

[48] K. Okamoto, B.T. Eger, T. Nishino, S. Kondo, E.F. Pai, T. Nishino, An extremely potent inhibitor of xanthine oxidoreductase. Crystal structure of the enzyme-inhibitor complex and mechanism of inhibition, J Biol Chem, 278 (2003) 1848-1855.

[49] Visualizer A D S. Version 4. 5[J]. Softw. Vis. Anal. Protein Struct, 2017.

[50] W. L. Wang, S. Y. Sheu, W. D. Huang,Y. L. Chuang, H. C. Tseng, T. S. Hwang, Y. T. Fu, Y. H. Kuo, C. H. Yao, T. F. Kuo, Phytochemicals from Tradescantia albiflora Kunth extracts reduce serum uric acid levels in oxonate-induced rats, Pharmacognosy magazine, 12 (2016) 223-227.

Graphical Abstract

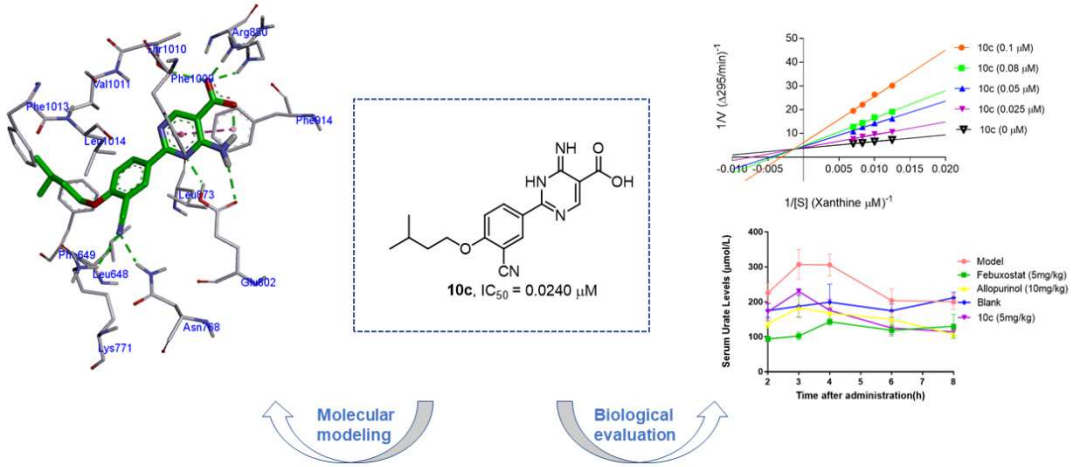

Highlights

•2-(4-alkoxy-3-cyano)phenyl-6-oxo-1,6-dihydropyrimidine-5-carboxylic acid derivatives were synthesized.

• **10c** and **10e** showed excellent XO inhibitory potencies with IC_{50} values of 0.0240 μM and 0.0181 μM.

• The structure-activity relationships of the synthesized compounds were summarized.

• Molecular modeling studies and steady-state kinetic analysis were performed.

• **10c** exhibited hypouricemic potency in potassium oxonate induced hyperuricemia rats.